Advances in Modeling Dielectric Breakdown

J. P. Verboncoeur

University of California, Berkeley

This work was supported in part by AFOSR (Counter High Power Microwave Consortium, and Cathodes and Breakdown MURI), and DOE (Insulator Breakdown STTR). Key researchers include Dr. S. K. Nam, Dr. H. C. Kim, M. Aldan, and S. Taverniers.

Single-Surface RF Multipactor

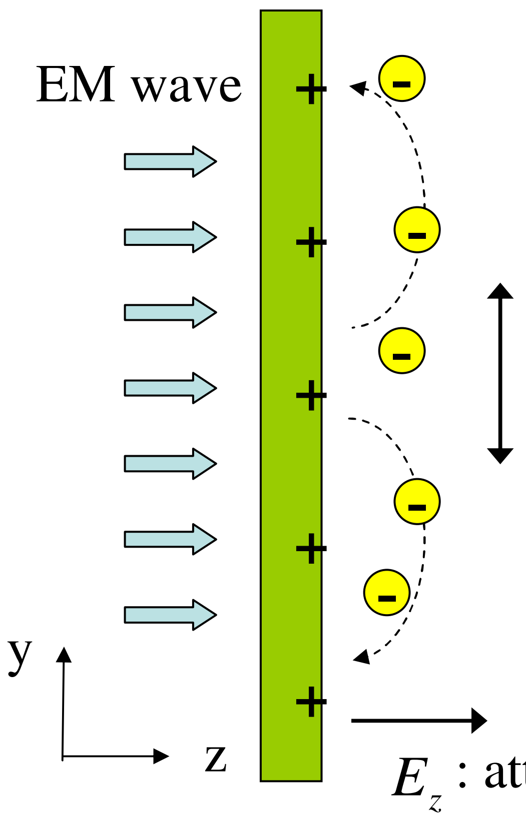

- <u>Multipactor discharge</u> is a <u>secondary electron avalanche</u> frequently observed in microwave systems.

$E_y = E_{rf0} \sin(\omega t)$: leads to electron energy gain.

E_z : attracts electrons

Dielectric Window

$$\tau_{transit} = 2m\,v_{z,0} / eE_{z0}$$ (life time)

$$z_{transit} = \frac{m}{2} \frac{v_{z,0}^2}{eE_{z0}}$$ (maximum distance)

$$E_{iy} = f\,(E_{rf0}/\omega,\ \omega\tau_{transit}, \phi_0 = \omega t_0)$$

Dominates at low pressure

Secondary Electron Model

- Energy and angular dependence of secondary emission coefficient

$$\delta(E_i,\theta)=\delta_{\max 0}\left(1+\frac{k_{s\delta}\theta^2}{2\pi}\right)\begin{cases}(we^{1-w})^k, & w\le 3.6\\ \dfrac{1.125}{w^{0.35}}, & w>3.6\end{cases}$$

$$w=\frac{E_i-E_0}{E_{\max 0}(1+k_{sw}\theta^2/2\pi)-E_0}$$

$$k=\begin{cases}0.56, & w<1\\ 0.25, & 1\le w\le 3.6\end{cases}$$

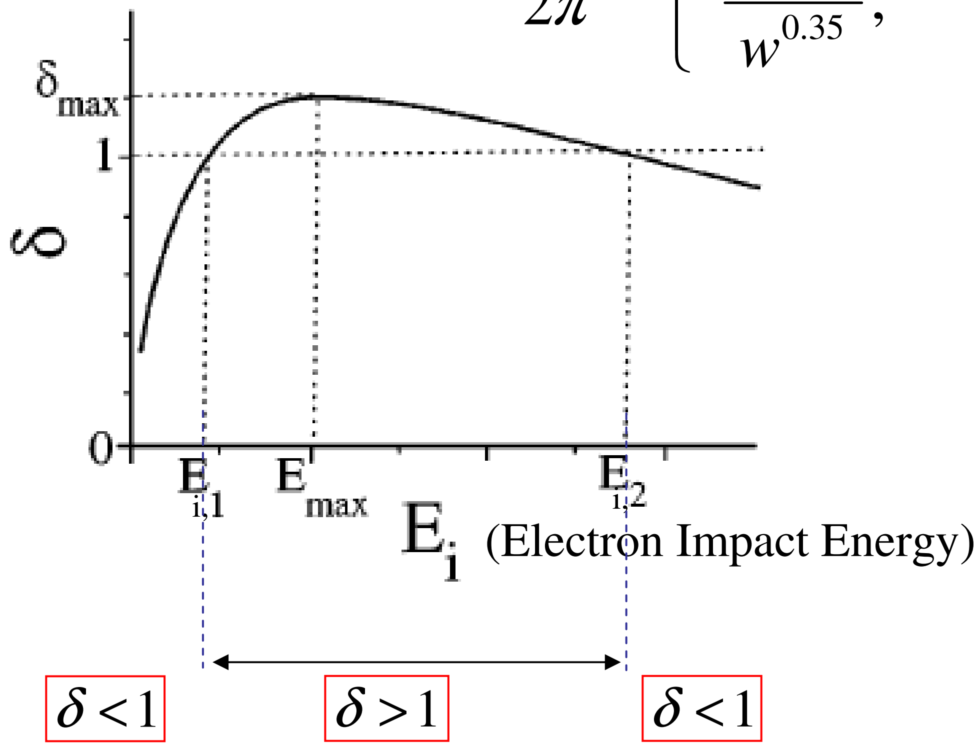

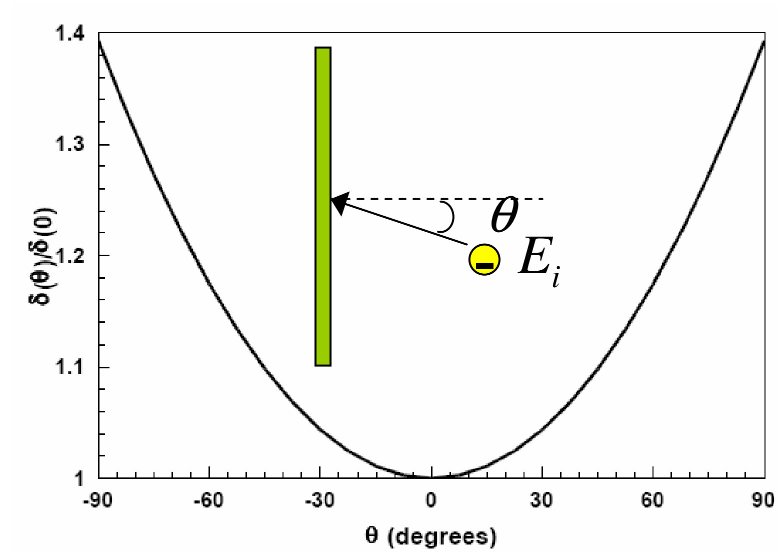

θ (Electron Impact Angle)

Vaughan *et al*, IEEE-TED (1989); IEEE-TED (1993)

PIC Multipactor Susceptibility

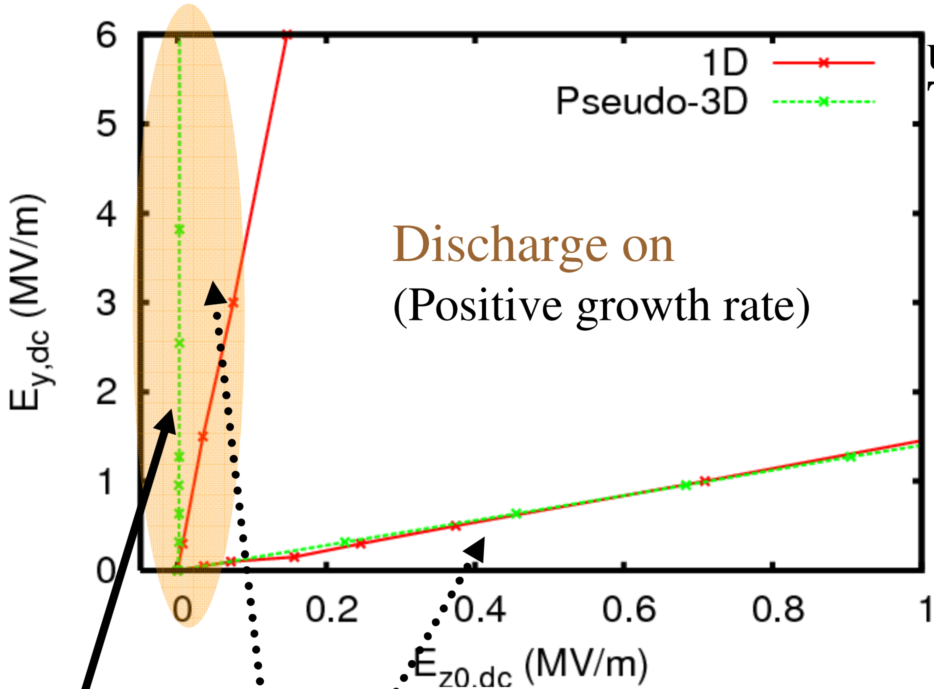

uniform plane wave
TE10 rectangular waveguide

- include transverse variation of E_{RF}
- absorb at transverse wall
- neglect transverse space charge

Discharge off : low δ due to
- Too high impact energy
- Too small impact energy

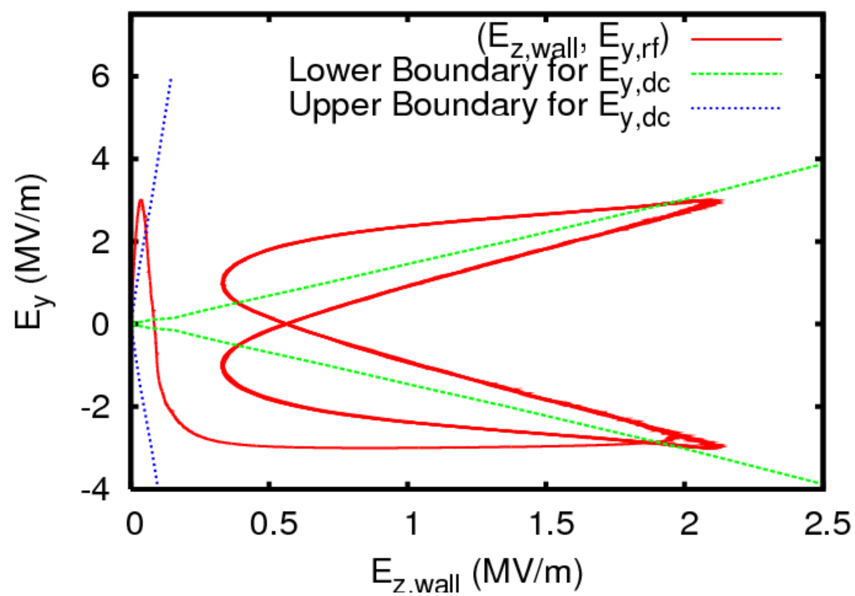

high field susceptibility becomes vertical in waveguide – no upper field cutoff

TE_{10} Multipactor Migration

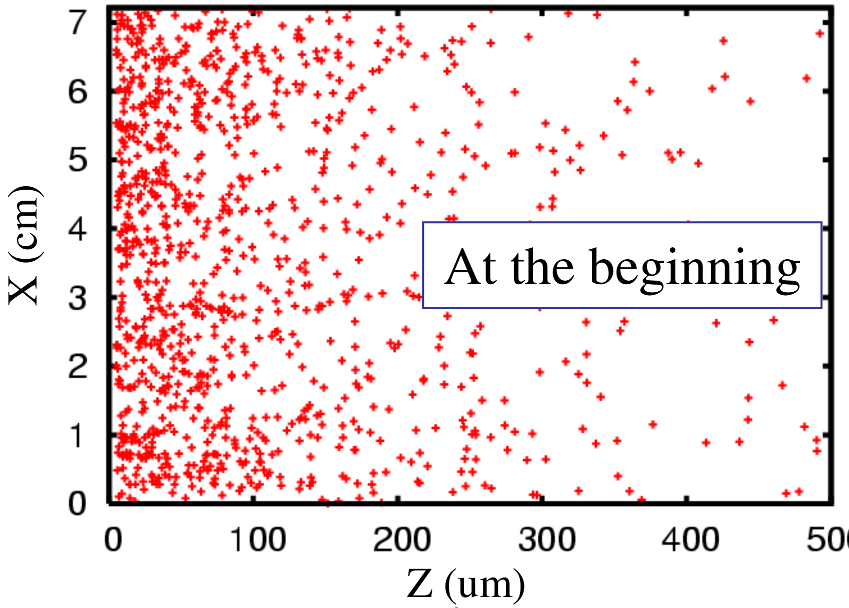

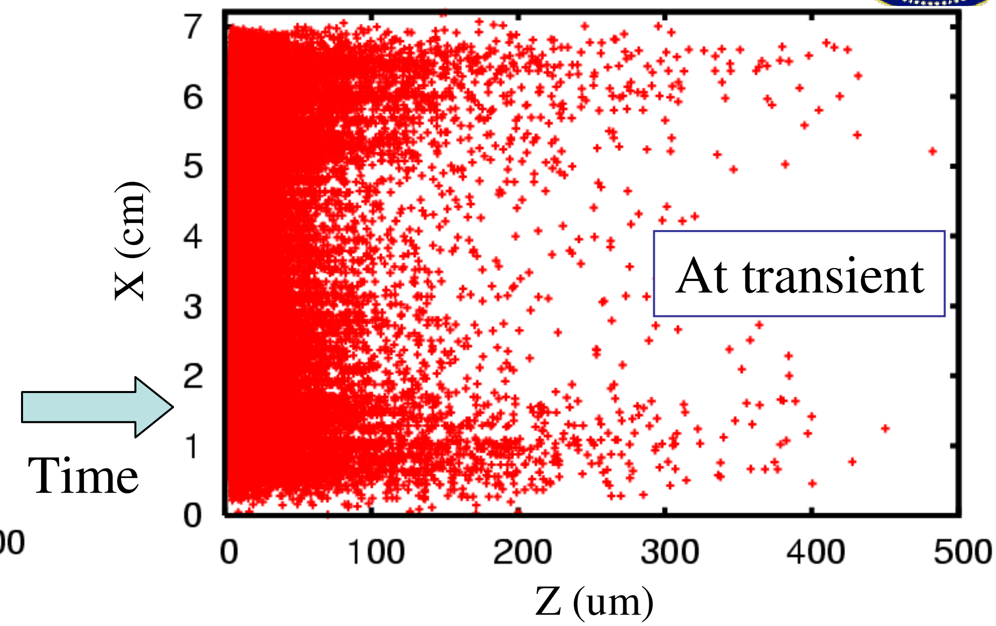

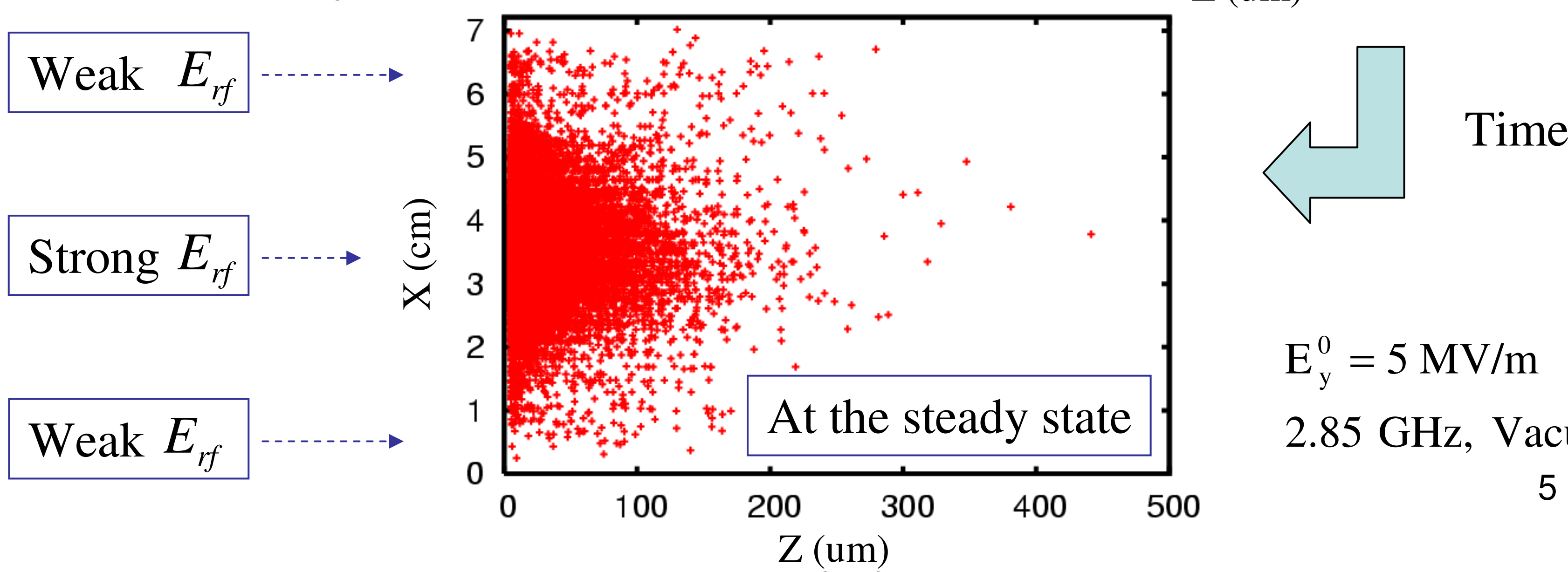

$E_y^0 = 5$ MV/m

2.85 GHz, Vacuum

Explanation of Migration

- Susceptibility Curve

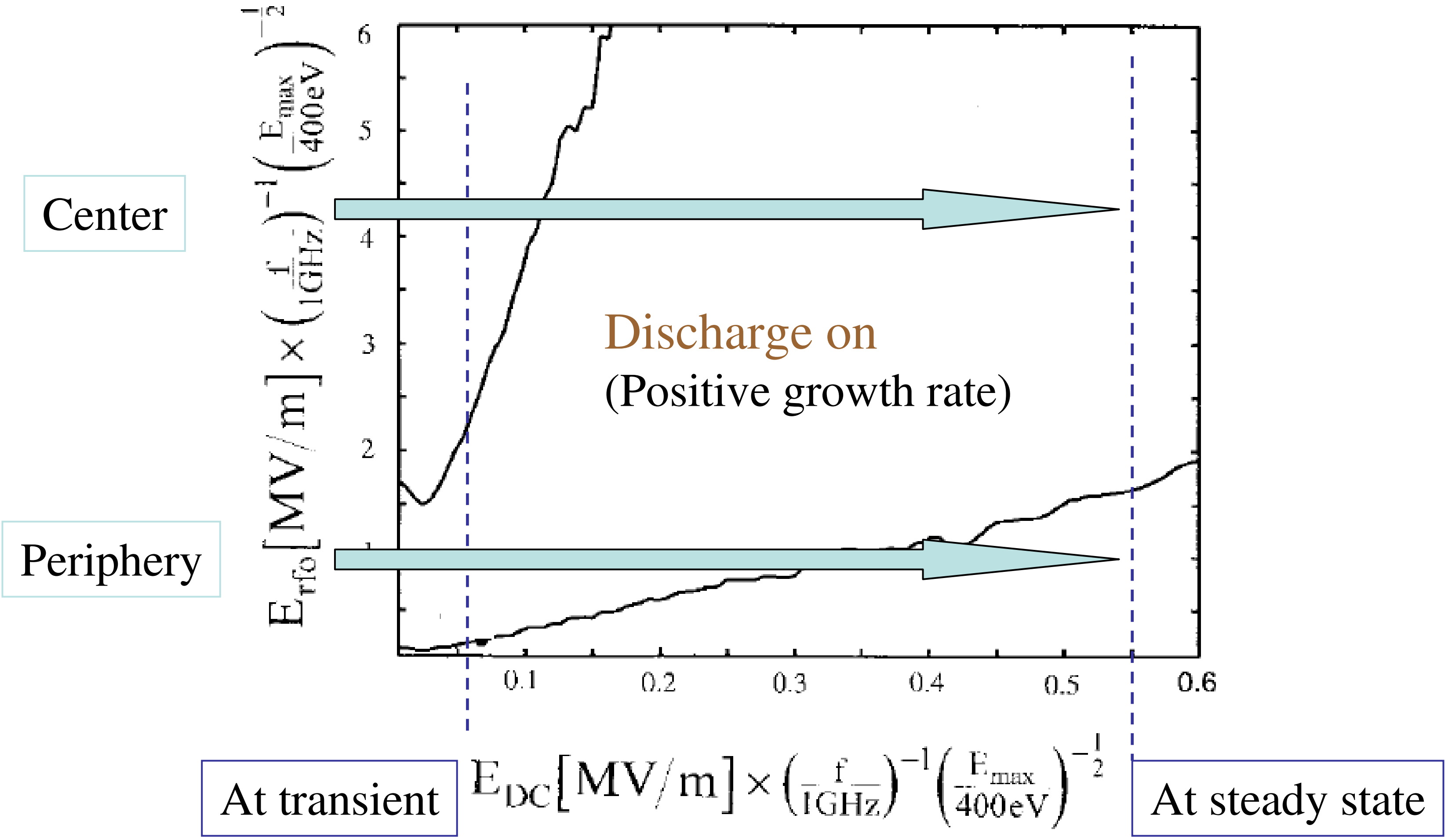

Multipactor Power

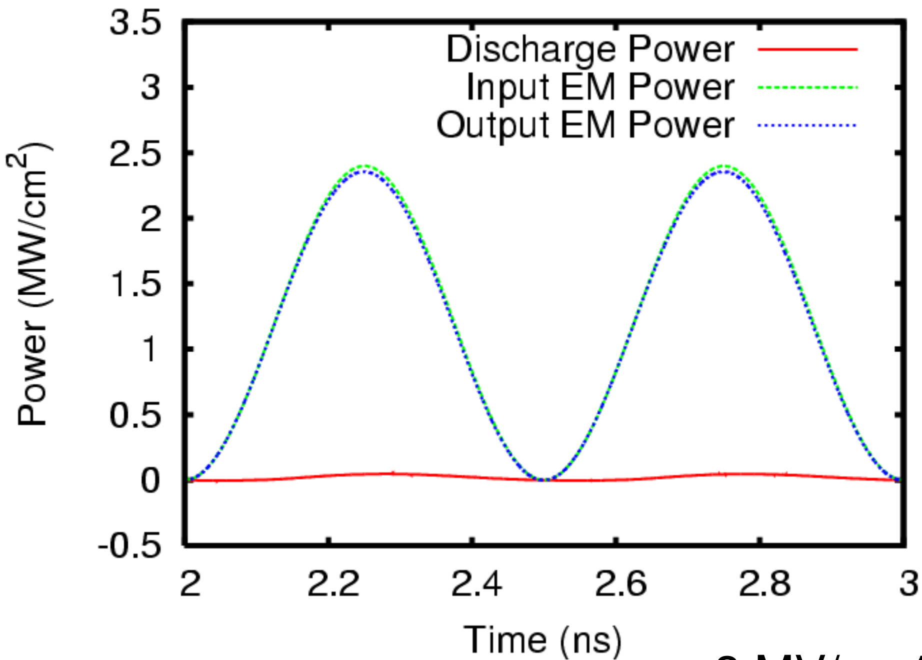

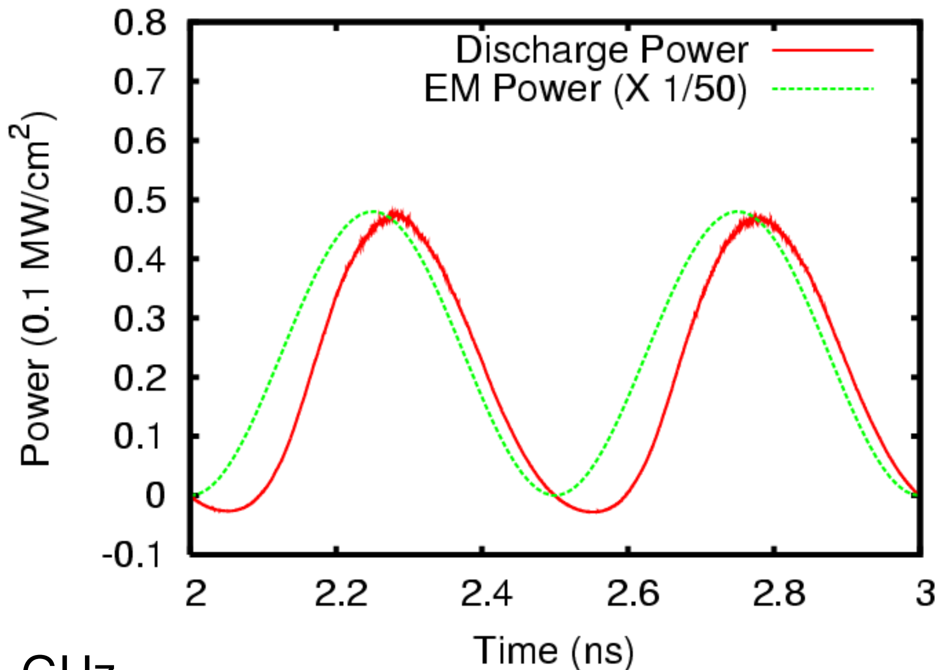

3 MV/m, 1 GHz

- ~2 % of the input EM power is absorbed
- The phase difference between the discharge power and input EM power means that the electrons are not totally in equilibrium with the local rf electric field.

Collisional Effects

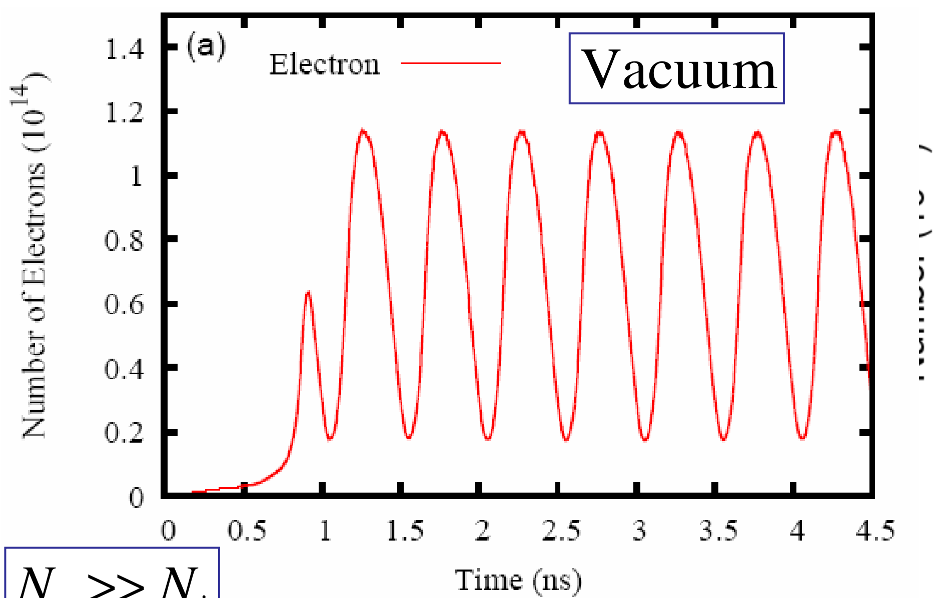

$N_e >> N_i$

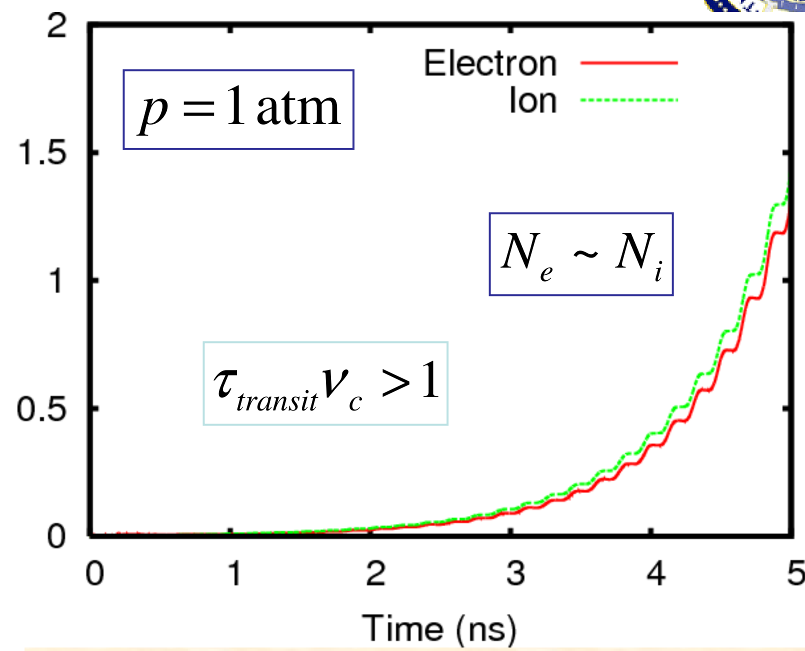

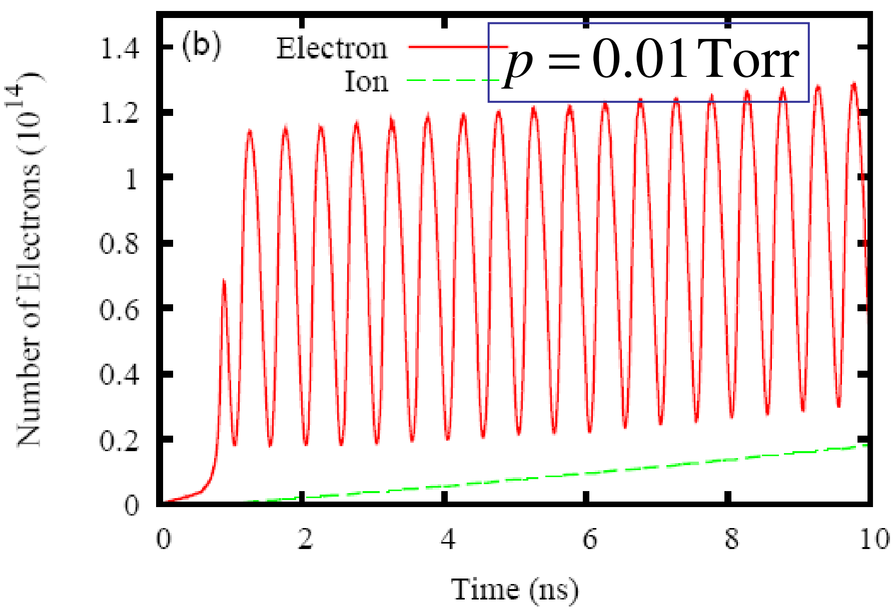

- As the pressure increases, electron-impact ionization collisions dominate secondary electron emission as the electron source.
- At high pressures, the number of ions becomes comparable to that of electrons.

$E_{rf0} = 3\,\mathrm{MV/m}$ at 1 GHz, Argon

PIC: Electron Mean Energy

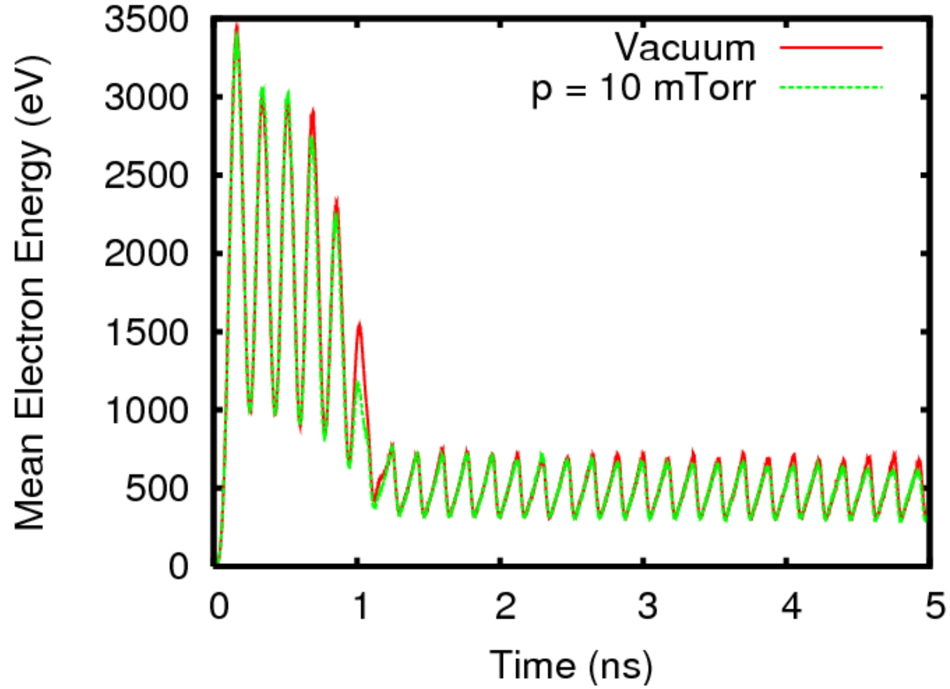

Vacuum and $p = 10\,\mathrm{mTorr}$

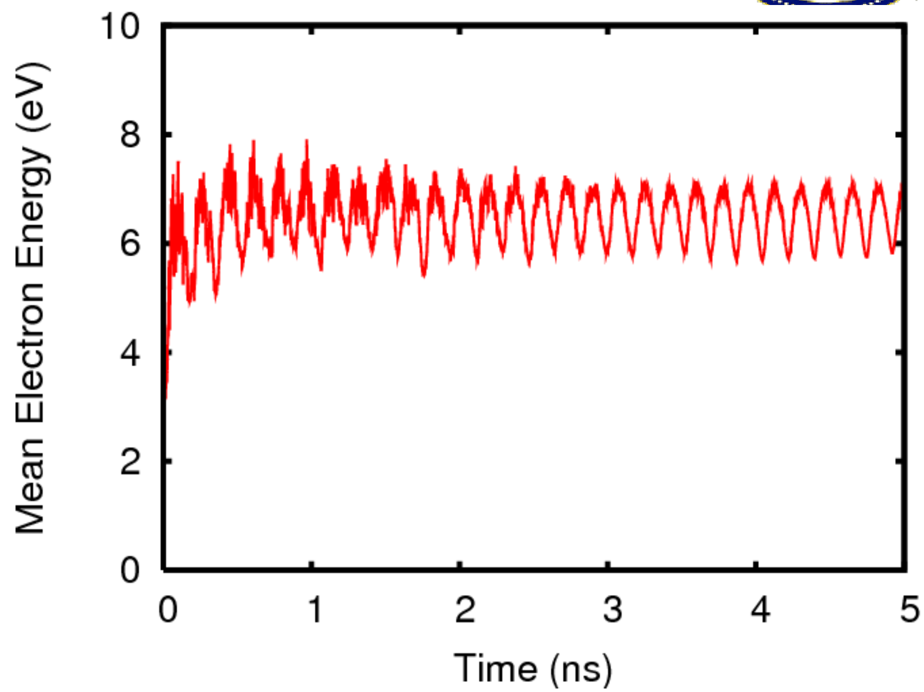

$p = 1\ \mathrm{atm}$

- Electrons in the multipactor discharge gain their energy by being accelerated by <u>the rf electric field during the transit time</u>.

- At high pressures, electrons <u>suffer many collisions</u> and lose a significant amount of energy gained from the rf electric field.

$E_{rf0} = 2.82\,\mathrm{MV/m}$ at $2.85\,\mathrm{GHz}$, Argon

Density Profile at Transition (1 Torr)

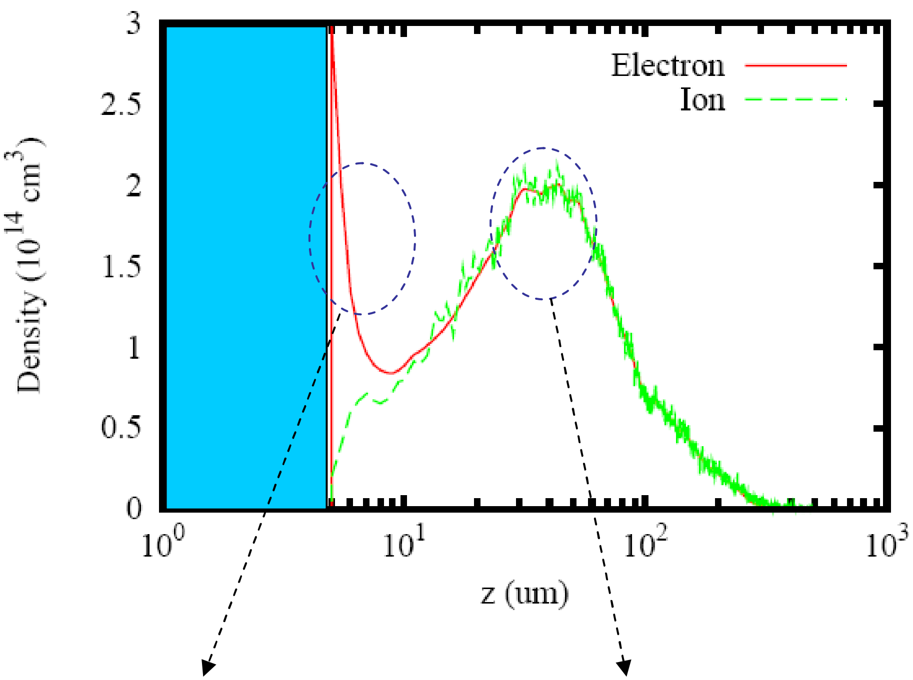

surface discharge from secondary emission: $\tau_{trans}\nu_c << 1$

volume discharge (rf plasma) from ionization

• High-velocity electrons generated from the secondary emission can reach the volume discharge region.

Secondary Yield vs. Pressure

Transition Pressure (10~50 Torr)

$\omega \geq \nu_c$

$\omega \tau_{transit,avg} < 1$

$\tau_{transit} \nu_c < 1$

surface discharge is collisionless.

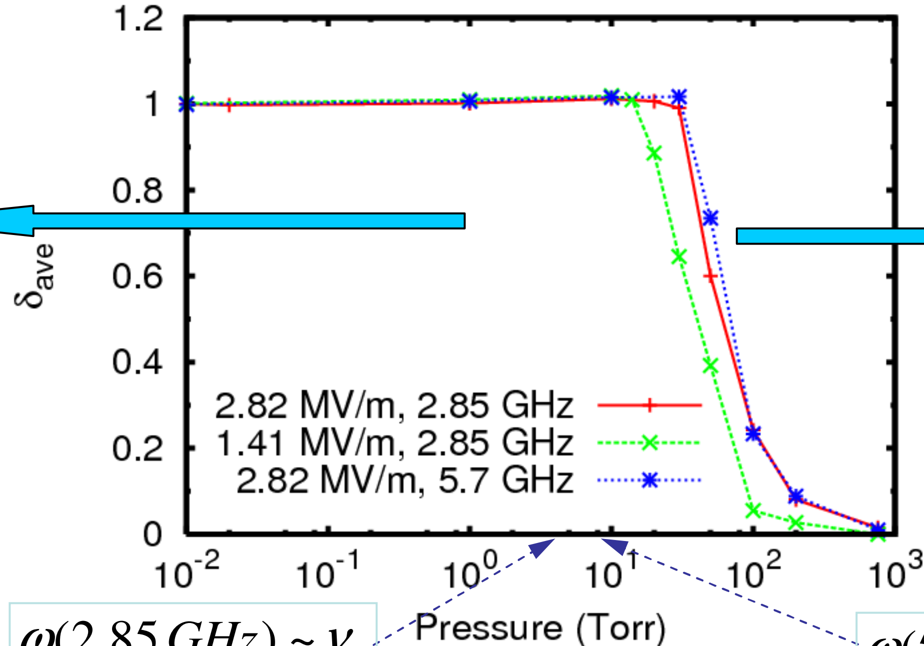

$\omega(2.85\ GHz) \sim \nu_c$

$\omega(5.7\ GHz) \sim \nu_c$

$\omega < \nu_c$

EEPF of rf plasma is Druyvesteyn.

- Below 10 Torr, the secondary yield is nearly unity so that secondary electron emission is sustained by itself.
- As the pressure increases and hence the volume discharge suppresses the secondary electron emission, it decreases to less than unity.

* For particles accumulated over a cycle

PIC: Electron Energy Distribution

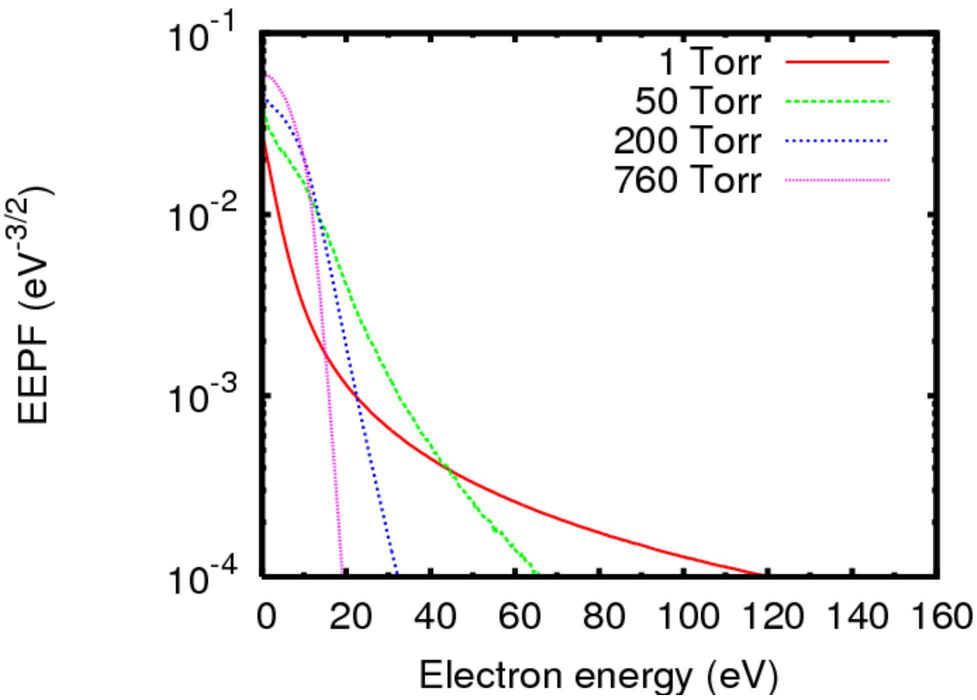

Spatially averaged

- Below 50 Torr, the EEPF is bi-Maxwellian like
- At high pressures, the EEPF becomes cutoff, with the depletion of high-energy electrons $\nu_c > \omega$

$E_{rf0} = 2.82\,\text{MV/m at } 2.85\,\text{GHz, Argon}$

TE_{10} Mode Effects

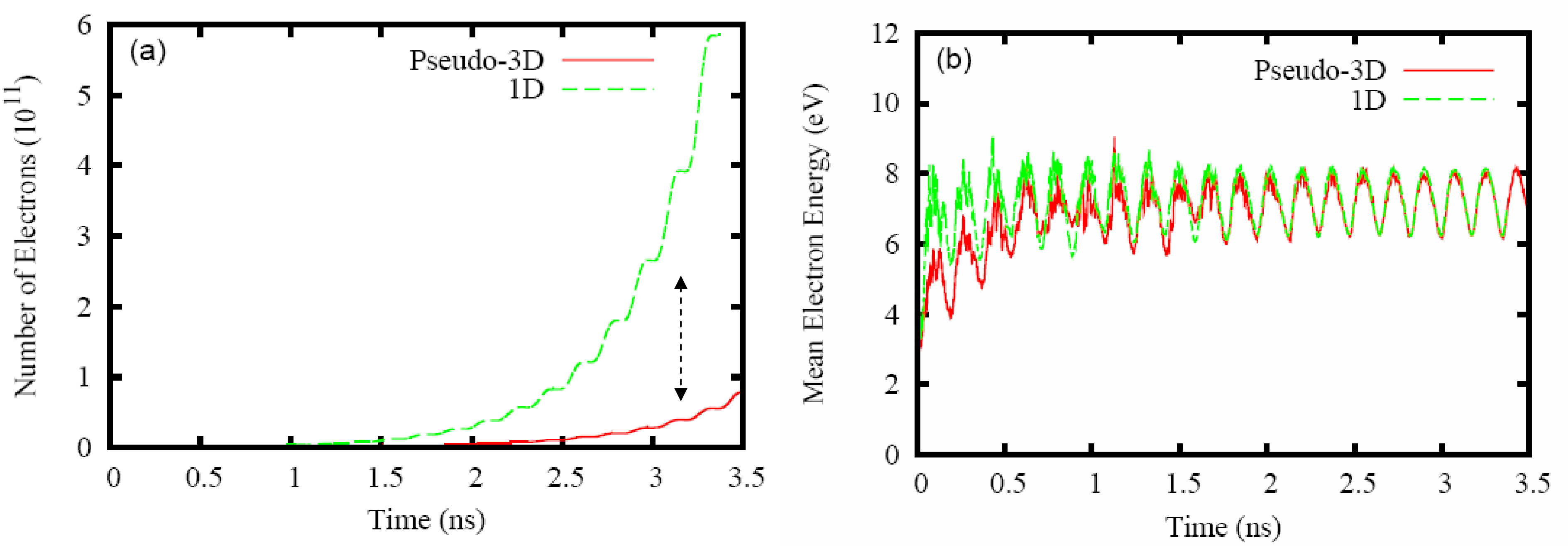

- Significant transverse loss of electrons to waveguide
- Lower growth rate
- Electron kinetic energy is not changed.

$E_y^0 = 1.41\,\text{MV/m}$

$2.85\,\text{GHz},\ 200\,\text{Torr}$

Breakdown Time: Gas Dependence

τ defined by $\dfrac{N(\tau)}{N(0)} = 10^8$

$E_{rf0} = 2.82\,\text{MV/m at }\ 2.85\,\text{GHz}$

τ vs. p

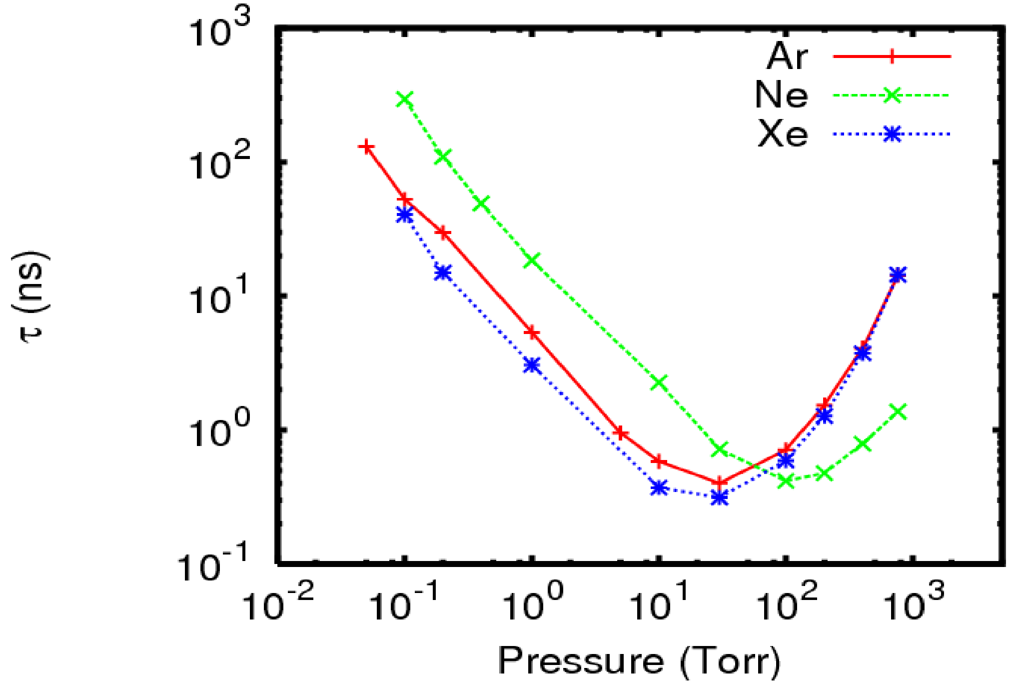

- Low pressure: τ for xenon is the lowest, due to largest ionization frequency
- High pressure: τ for neon is the lowest, because the total frequency of collisions leading to significant electron energy loss is lowest in neon

Scaling Law: Low p

Postulate: $n(t)=n_0\exp(\langle\nu_i\rangle t)$, with the mean ionization rate $\langle\nu_i\rangle \sim \nu_{i,max}/2$

For $n(\tau)/n_0=10^8$, we obtain $\tau=18.4/\langle\nu\rangle$

At low p: $\frac{1}{\tau_f} >> \omega >> \nu_c$ with τ_f the electron flight time

Breakdown time: $\tau \sim \frac{1}{\nu_i} \sim \frac{1}{n_g\langle\sigma v\rangle} \sim \frac{1}{p}$

since $\langle\sigma v\rangle$ changes slowly near E~500 eV typical of low p regime

Then the scaling law predicts:

τ(Argon) ~ 6.4 ns/p(Torr),

τ(Neon) ~ 18 ns/p(Torr),

τ(Xenon) ~ 2 ns/p(Torr).

Lau, Verboncoeur, and Kim, **APL**, 89, 261501 (2006)

Scaling Law: High p

Ionization discharge regime, with $\omega << \nu$

Rate of change in electron KE: $\frac{dW}{dt} = \frac{e^2 E_0^2}{2m\nu_c} - \text{loss terms}$ with E_0 the rf electric field

Assume 50% of energy to loss terms, then

$$\tau = 6.8\times10^{-12}\,\text{s}\times\left(\frac{\overline{W}_i}{10\text{eV}}\right)\left(\frac{<\sigma v>_c}{10^{-13}\,\text{m}^3/\text{s}}\right)\left(\frac{p}{1\,\text{Torr}}\right)\left(\frac{1\text{MV/m}}{E_{eff}}\right)^2 \qquad E_{eff} \equiv \frac{E_{rf\,0}}{\sqrt{2[1+(\omega/\nu_c)^2]}}$$

Rearranging: $$\frac{E_{eff}}{p}\left(\frac{\text{V}}{\text{cm}-\text{Torr}}\right) = \frac{0.026}{\sqrt{\left(\frac{p\tau}{\text{Torr - s}}\right)}}\times\sqrt{\left(\frac{\overline{W}_i}{10\text{eV}}\right)\left(\frac{<\sigma v>_c}{10^{-13}\,\text{m}^3/\text{s}}\right)}$$

Scaling law predicts:

$$E_{eff}\,/\,p[\text{V/(cm}-\text{Torr)}] = 0.064/\sqrt{p\tau(\text{Torr}-\text{s})}; \qquad \text{Ar}$$

$$E_{eff}\,/\,p[\text{V/(cm}-\text{Torr)}] = 0.045/\sqrt{p\tau(\text{Torr}-\text{s})}; \qquad \text{Xe}$$

$$E_{eff}\,/\,p[\text{V/(cm}-\text{Torr)}] = 0.037/\sqrt{p\tau(\text{Torr}-\text{s})}; \qquad \text{Ne}$$

Lau, Verboncoeur, and Kim, **APL**, 89, 261501 (2006)

Breakdown Scaling Law

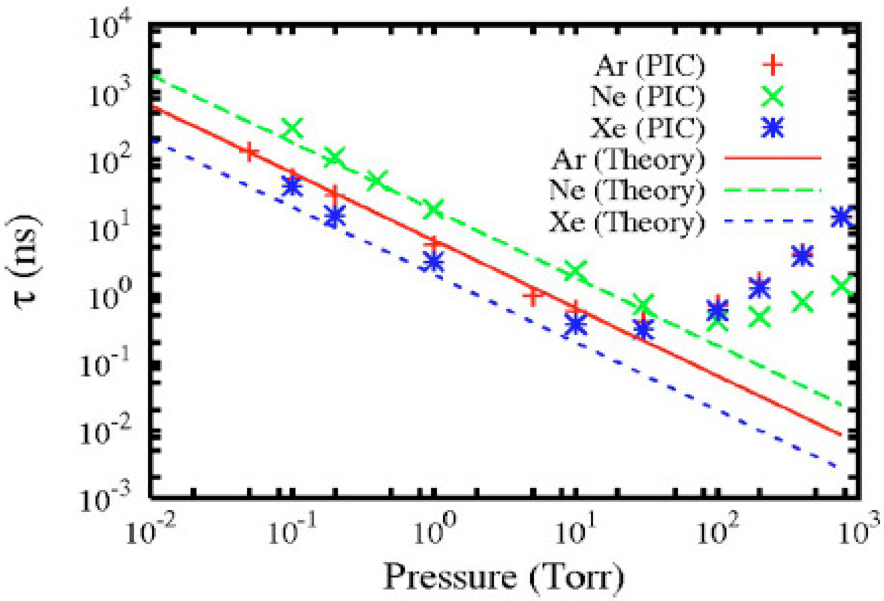

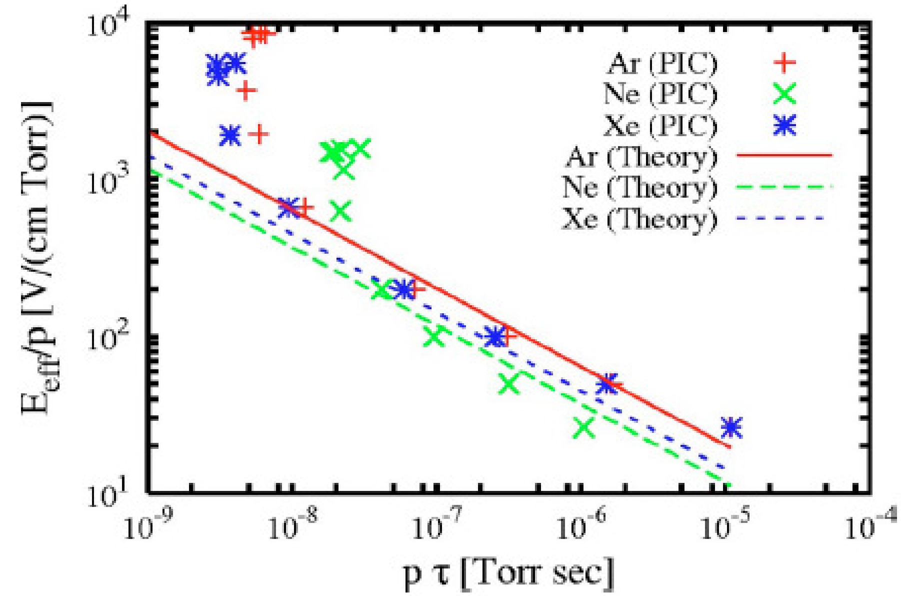

Low pressure regime:
surface multipactor dominated

$$\tau \sim \frac{1}{\nu_i} \sim \frac{1}{n_g \langle \sigma v \rangle} \sim \frac{1}{p}$$

High pressure regime:
collision dominated ($\nu_c >> \omega$)
volumetric discharge

$$\frac{E_{eff}}{p} \sim \frac{1}{\sqrt{p\tau}}$$

Lau, Verboncoeur, and Kim, **APL**, 89, 261501 (2006)

Enhanced Global Model* I

- Coupled continuity equations for all species, e.g. for oxygen:

$$\frac{dn_e}{dt} = K_{ion} n_e n_{gas} - K_{att} n_e n_{gas} - K_{rec} n_e n_{O_2^+} + K_{\det} n_e n_{O^-} + K_{\det 2} n_{O_2^+} n_{O^-}$$

$$\frac{dn_{O_2^+}}{dt} = K_{ion} n_e n_{gas} - K_{rec} n_e n_{O_2^+} - K_{mut} n_{O^-} n_{O_2^+}$$

$$\frac{dn_{O^-}}{dt} = K_{att} n_e n_{gas} - K_{\det} n_e n_{O^-} - K_{mut} n_{O^-} n_{O_2^+} - K_{\det 2} n_{O_2^+} n_{O^-}$$

where $K = \int_\varepsilon \sqrt{\frac{2e\varepsilon}{m_e}} \sigma(\varepsilon) f(\varepsilon) d\varepsilon$

* Nam and Verboncoeur, *APL* **23**, 231502 (2008)

Oxygen Reactions

$1)\ e + O_2 \rightarrow e + O_2$

$2)\ e + O_2 \rightarrow e + O_2(r)$

$3\text{-}6)\ e + O_2 \rightarrow e + O_2(\upsilon = n, n = 1,2,3,4)$

$7)\ e + O_2 \rightarrow e + O_2(a^1\Delta_g)$

$8)\ e + O_2 \rightarrow e + O_2(b^1\Sigma_g^+)$

$9)\ e + O_2 \rightarrow O + O^-$

$10)\ e + O_2 \rightarrow e + O_2(c^1\Sigma_u^-, A^3\Sigma_u^+)$

$11)\ e + O_2 \rightarrow e + O(3P) + O(3P)$

$12)\ e + O_2 \rightarrow e + O(3P) + O(1D)$

$13)\ e + O_2 \rightarrow e + O(1D) + O(1D)$

$14)\ e + O_2 \rightarrow e + O_2^+ + e$

$15)\ e + O_2 \rightarrow e + O + O^*(3p^3P)$

$16)\ e + O_2^+ \rightarrow O + O$

$17)\ e + O^- \rightarrow e + O + e$

$18)\ O^- + O_2^+ \rightarrow O + O_2$

$19)\ O^- + O_2 \rightarrow O + O_2 + e$

Enhanced Global Model II

- Electron energy equation:

$$\frac{d}{dt}\left(\frac{3}{2}n_e kT_{eff}\right) = P_{abs} - (\varepsilon_{ion}K_{ion}n_e n_{gas} + \sum_{exc}\varepsilon_{exc}K_{exc}n_e n_{gas} + \tilde{K}_{mom}n_e n_{gas})$$

- Improved RF power absorption model:

$$P_{abs} = \int \frac{e^2 n_e}{m\nu_m}\left(\frac{E_0}{\sqrt{2}}\frac{\nu_m}{\sqrt{\nu_m^2+\omega^2}}\right)^2 f(\varepsilon)d\varepsilon$$

Enhanced Global Model III

- The general EEDF equation in the isotropic velocity space *:

$$f(\varepsilon) = c_1 \varepsilon^{1/2} e^{-c_2 \varepsilon^x}$$

- Maxwellian: x=1, Druyvestyn: x=2
- Determine x by the ionization and dissociative attachment from PIC model:

$$K_{ion}\big|_{PIC} - K_{att}\big|_{PIC} =$$

$$\int_{\varepsilon_{\rm ion}} \sqrt{\frac{2e\varepsilon}{m_e}} \cdot \sigma_{ion}(\varepsilon) \cdot c_1 \varepsilon^{1/2} e^{-c\left(\frac{\varepsilon}{T_{eff}}\right)^x} d\varepsilon - \int_{\varepsilon_{\rm att}} \sqrt{\frac{2e\varepsilon}{m_e}} \cdot \sigma_{att}(\varepsilon) \cdot c_1 \varepsilon^{1/2} e^{-c\left(\frac{\varepsilon}{T_{eff}}\right)^x} d\varepsilon$$

* J. T. Gudmundsson, *Plasma Sources Sci. Technol.*, **10**, 76 (2001).

Enhanced Global Model in Ar

Argon Gas
E_o = 2.82 MV/m
f = 2.85 GHz

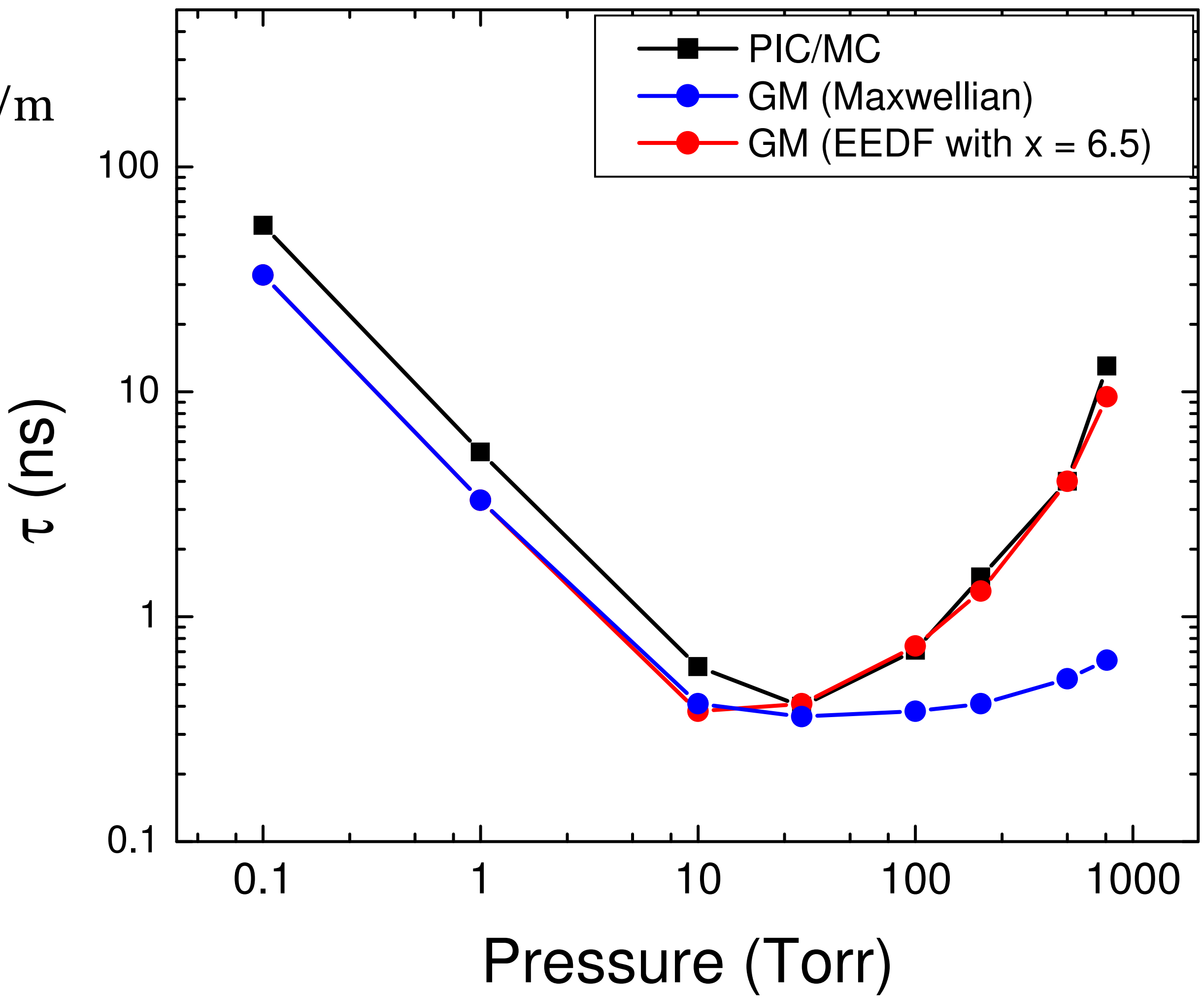

EEPF in Argon

Argon Gas
E_o = 2.82 MV/m
f = 2.85 GHz
p = 760 Torr

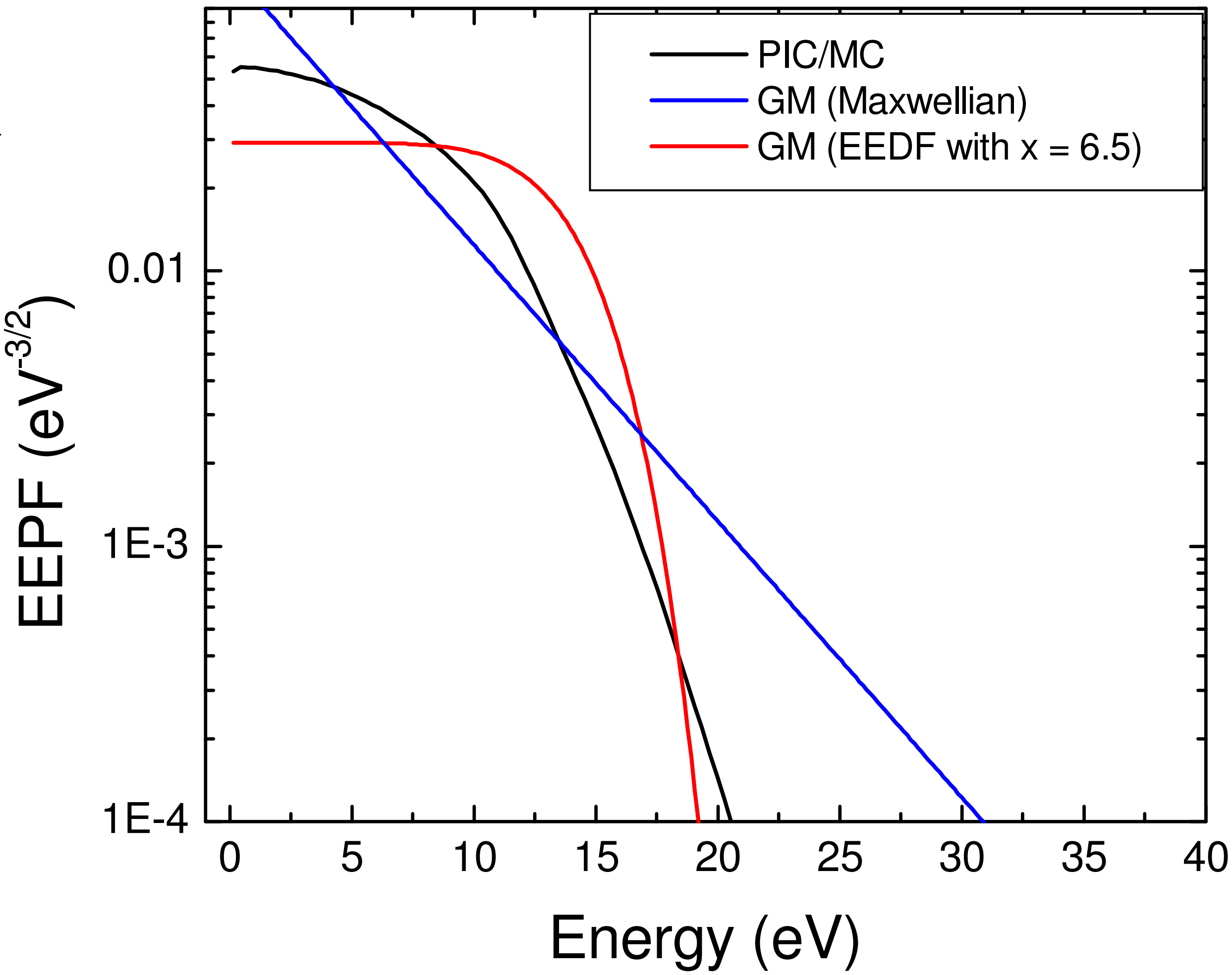

Breakdown time in oxygen

Oxygen
E_0 = 4.23 MV/m
f = 2.85 GHz

PIC/MC

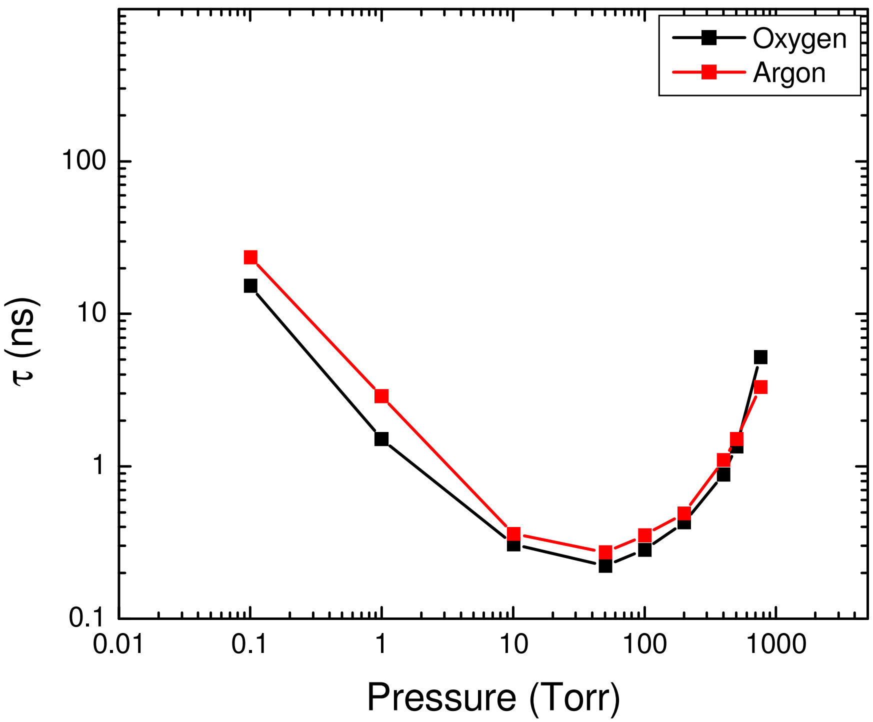

Global Model (GM)

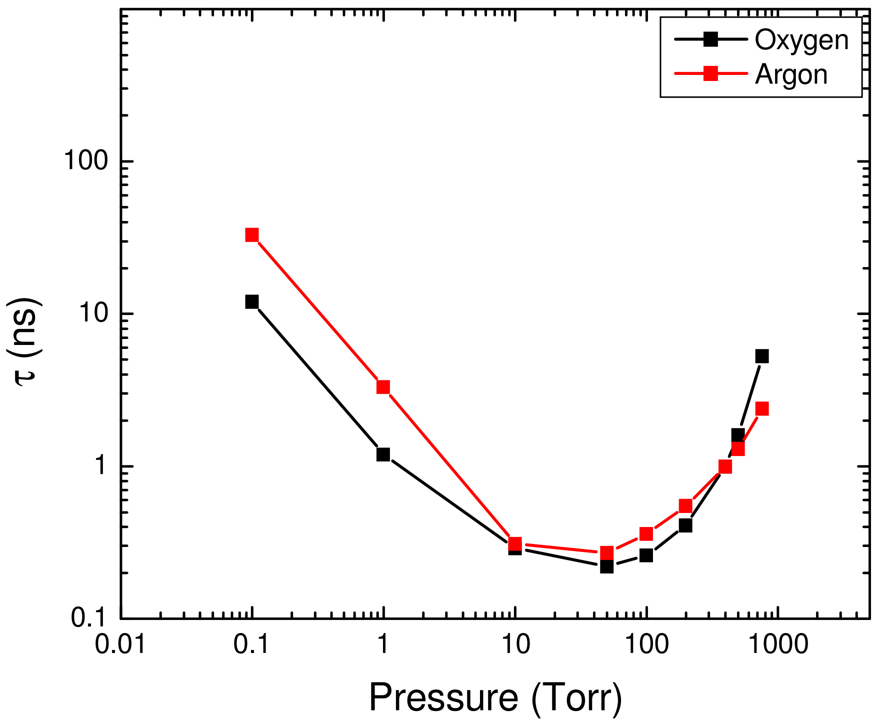

Breakdown Time in Air

Air
E_o = 4.23 MV/m

f = 2.85 GHz

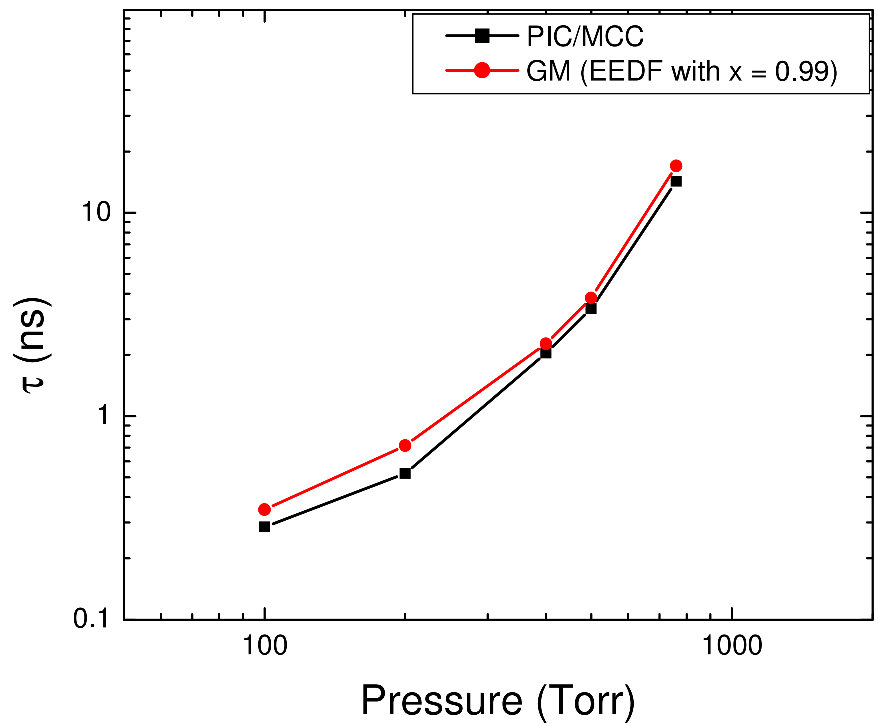

f = 5.70 GHz

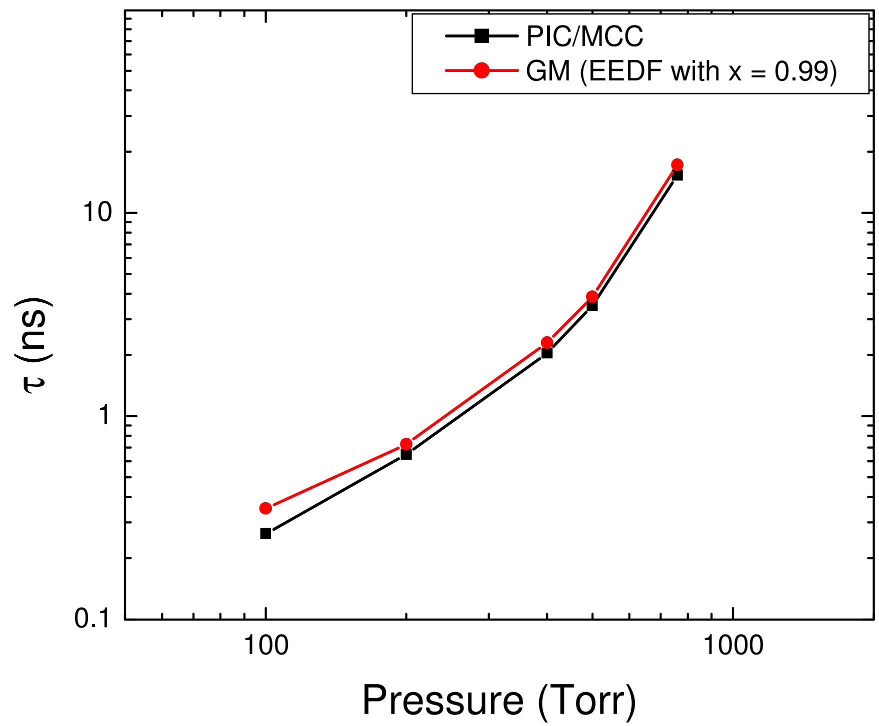

Energy loss rate and T_{eff}

E_o = 4.23 MV/m
f = 2.85 GHz

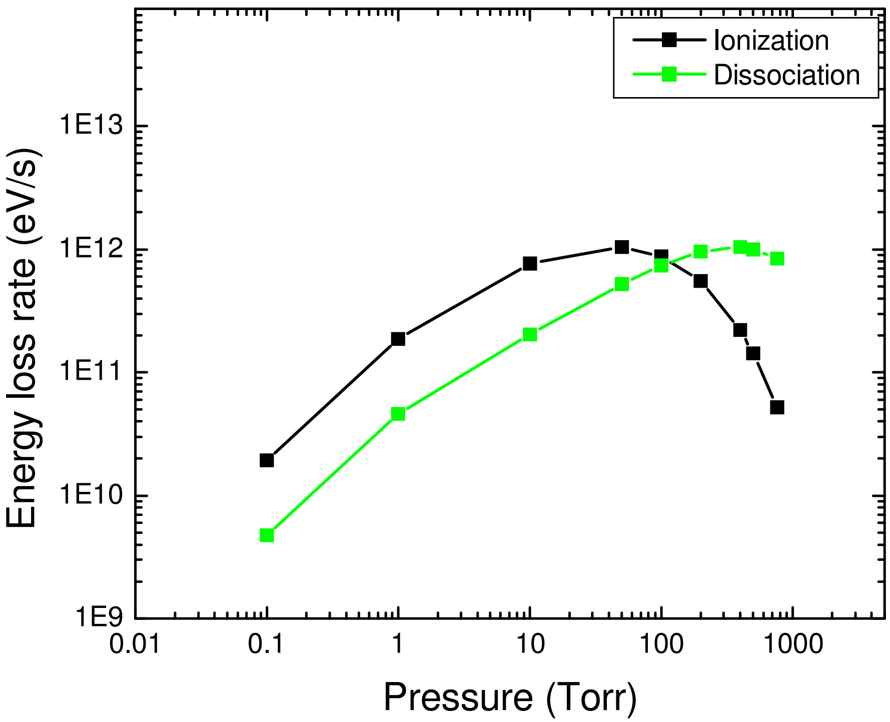

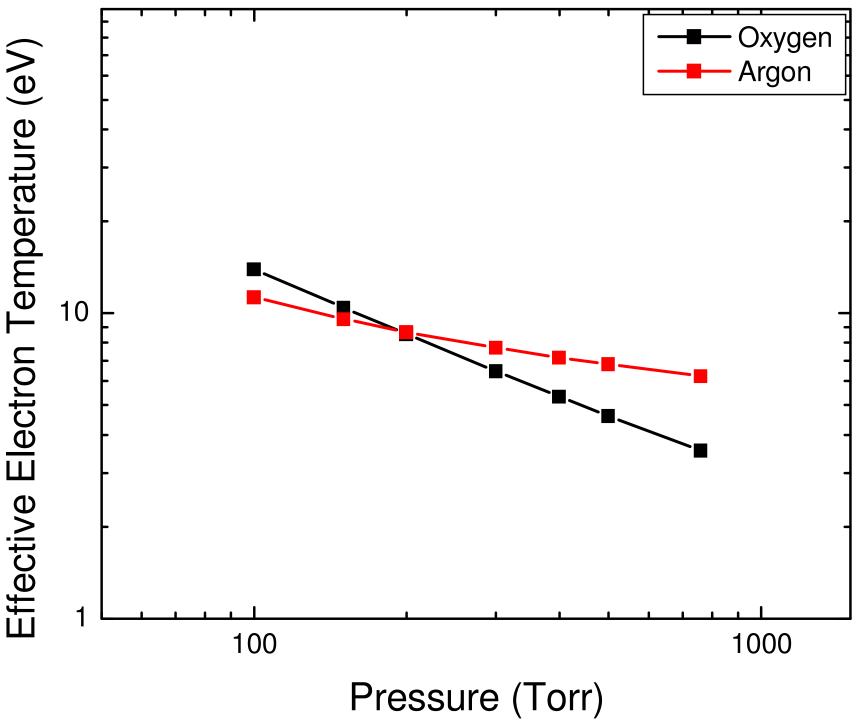

Applied E vs f for K_{ratio}=1 in air

$$K_{ratio} = \frac{K_{att}}{K_{ion}}$$

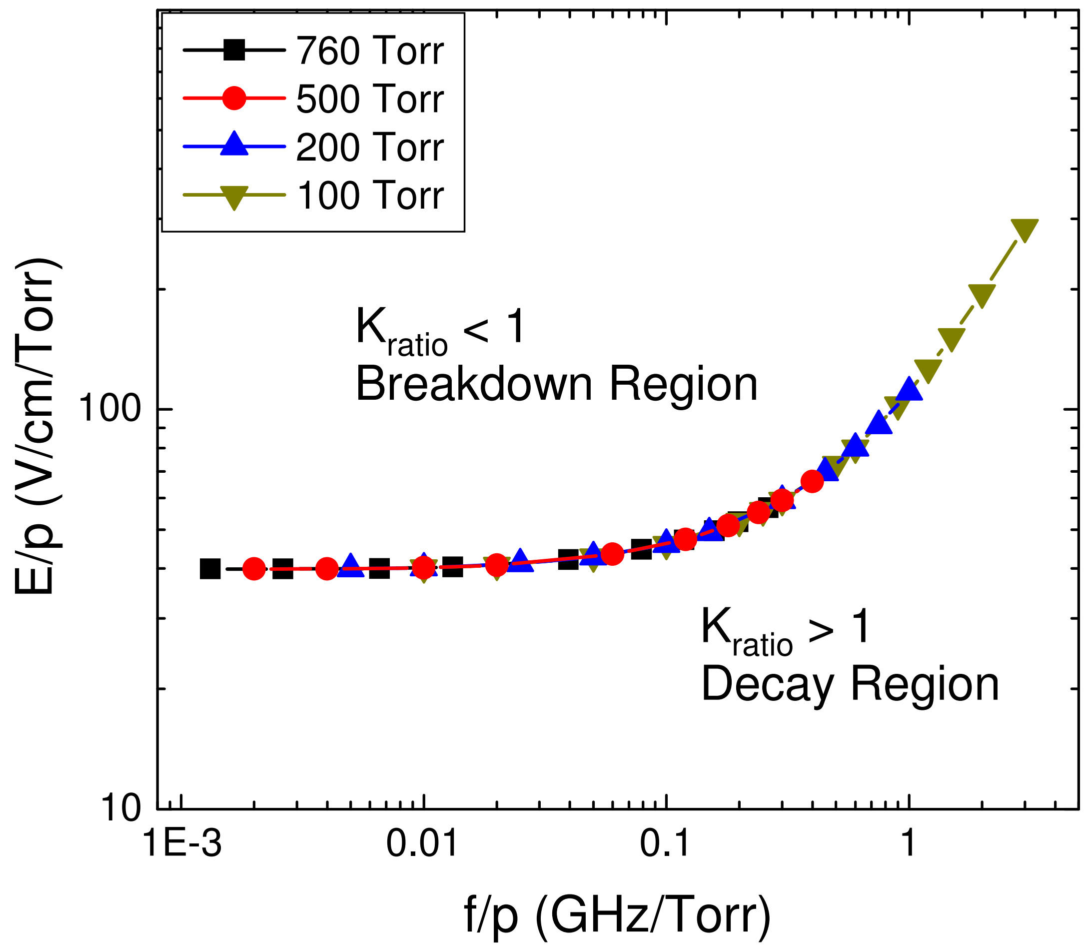

Effect of Frequency

Constant x is inadequate at high frequency for Ramsauer gases

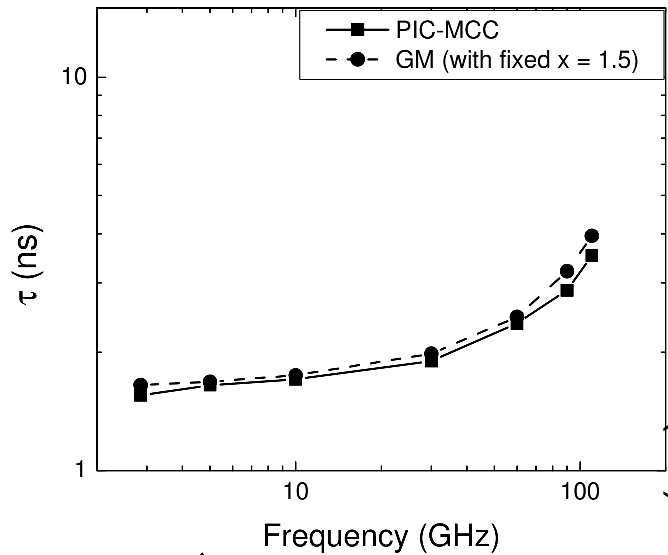

Oxygen

Argon

E_o = 2.82 MV/m

P =500 Torr

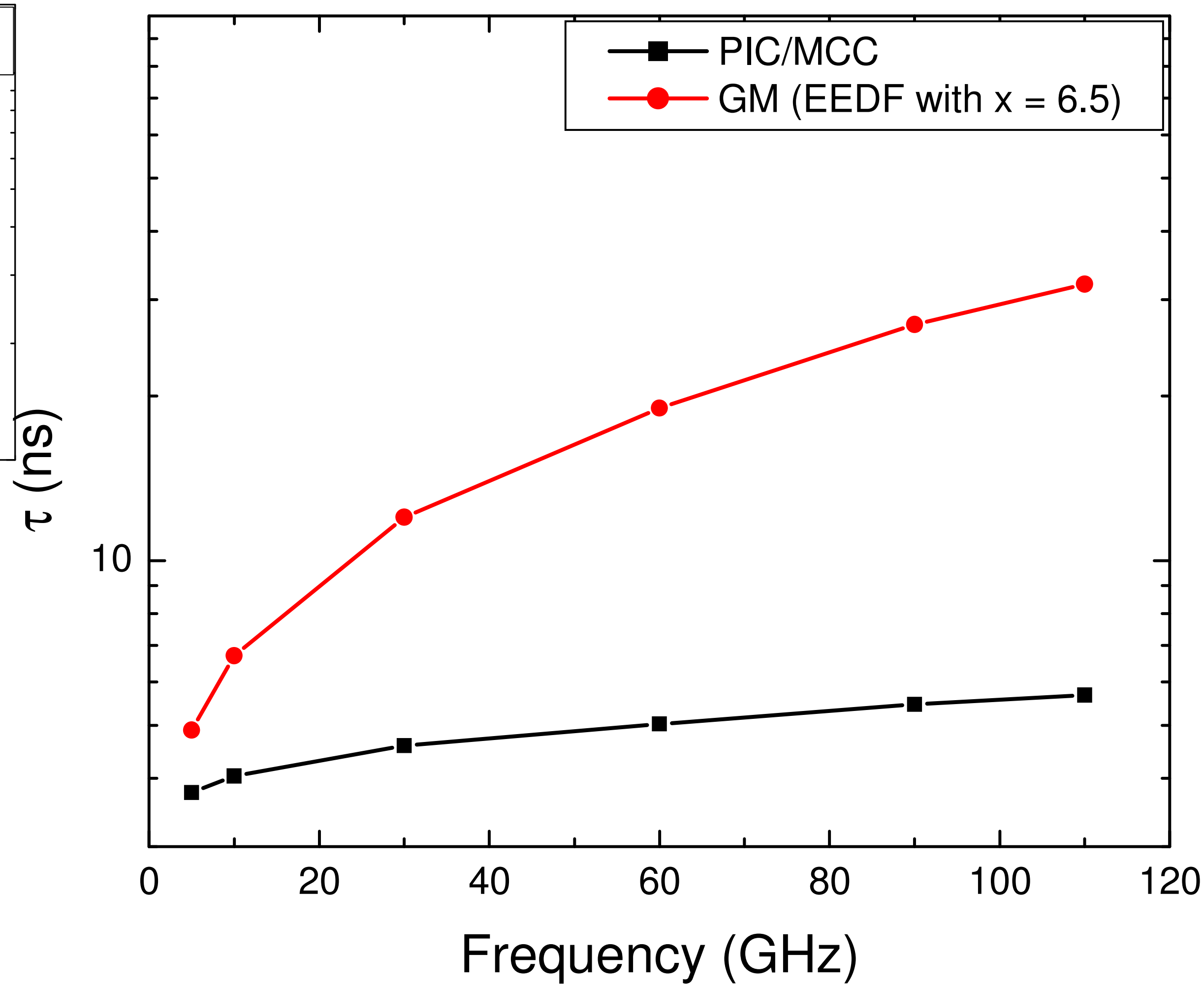

Effect of Frequency

Argon
E_0 = 2.82 MV/m, p=500 Torr
Xenon
E_0 = 2.82 MV/m, p = 700 Torr

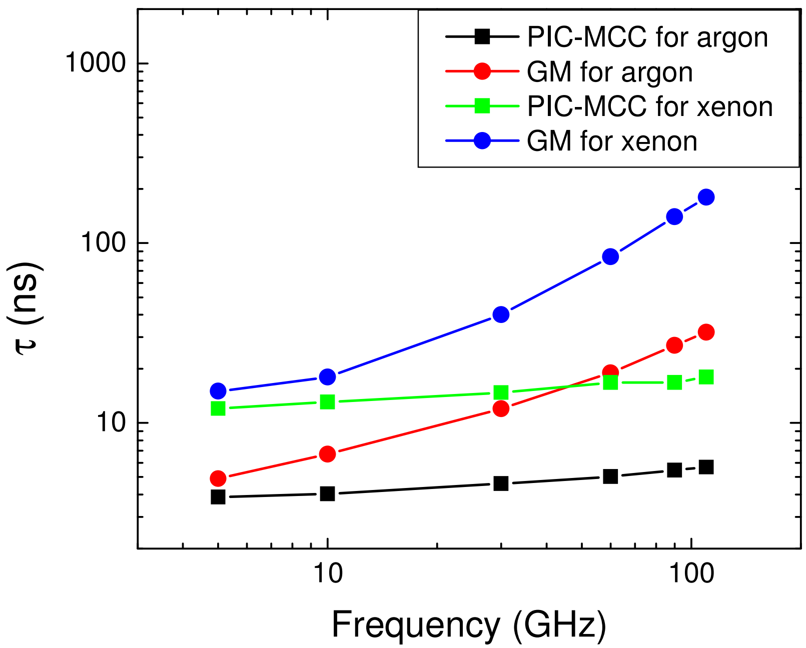

Oxygen and Nitrogen
E_0 = 4.23 MV/m
p = 500 Torr

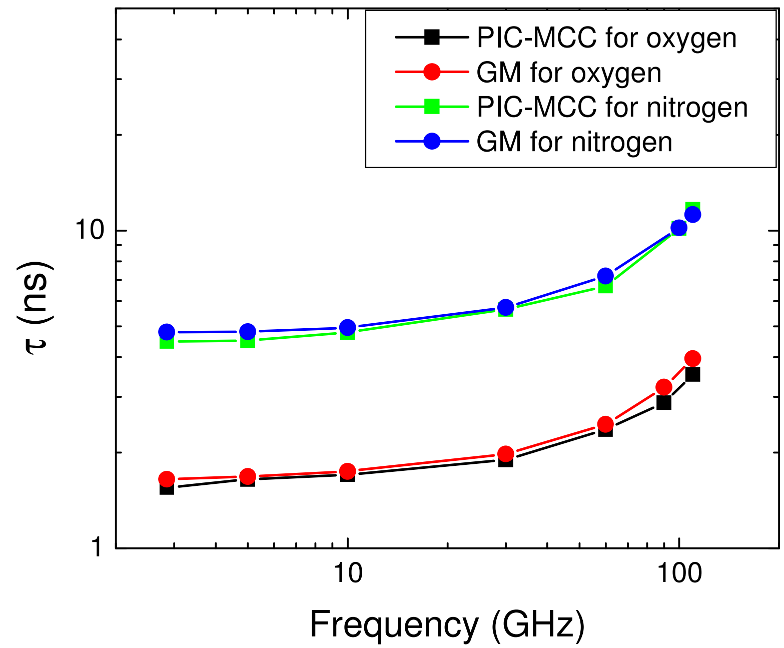

Sang Ki Nam and J. P. Verboncoeur, *Appl. Phys. Lett.*, **93**, 151504 (2008).

Argon: frequency dependence of x

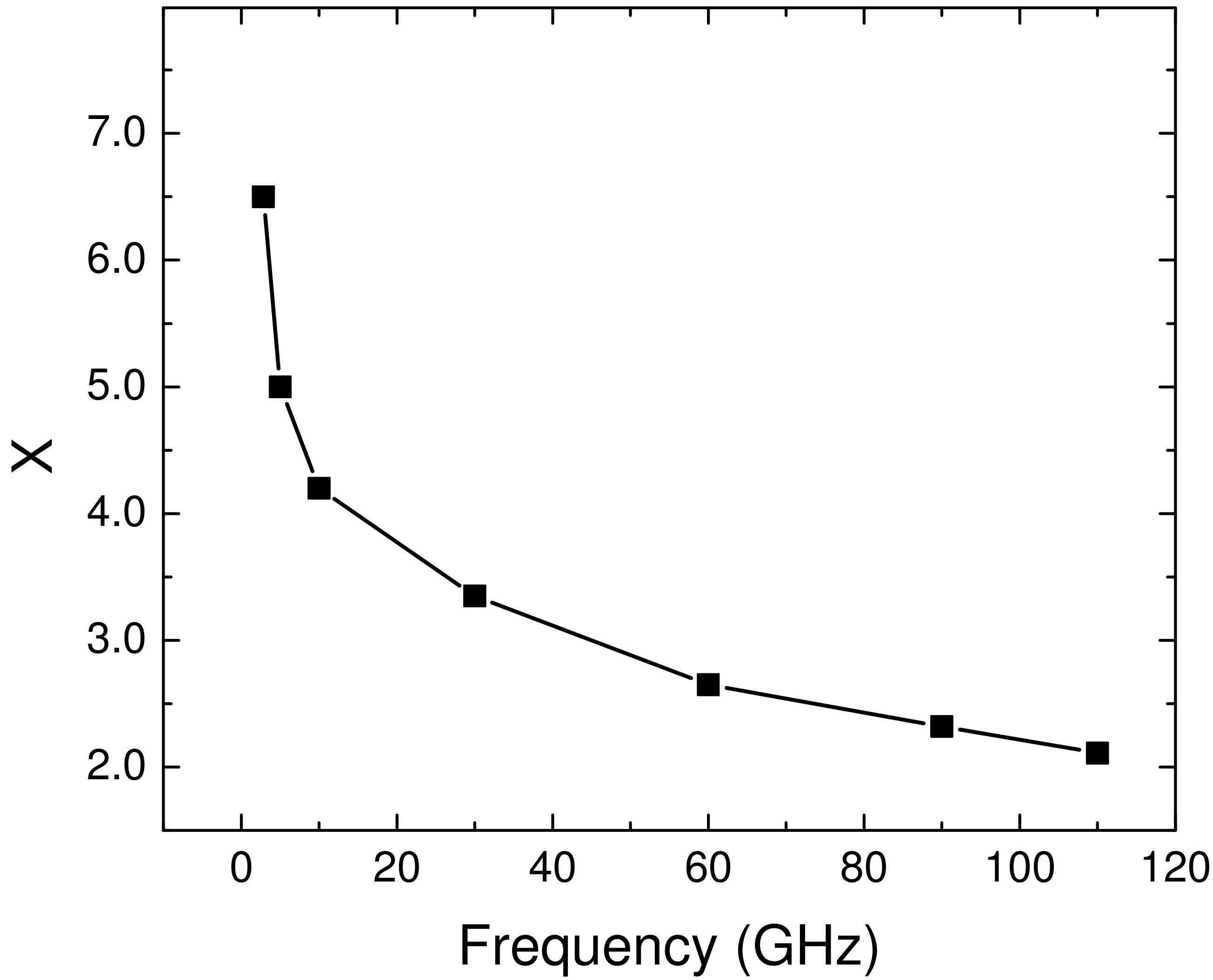

Comparison to Experiment

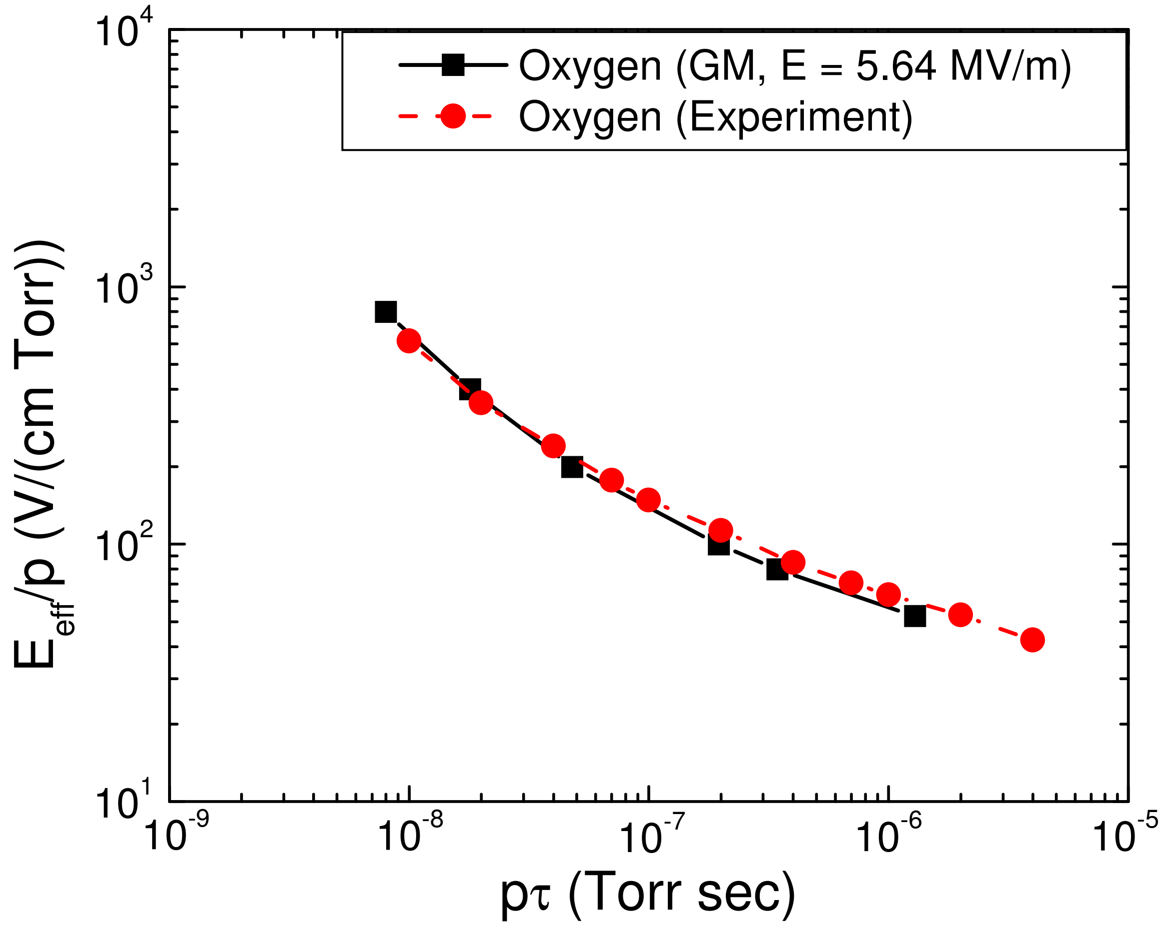

* P. Felsenthal and J. M. Proud, *Phys. Rev.*, **139**, A 1796 (1965).

Plasma Filamentary Arrays

- 1.5 MW, 140 GHz Gyrotron
- 3 shots with slow (B&W) and fast (color) cameras
- Filaments spaced slightly less than $\lambda/4$, propagate towards source
- Hypothesis: constructive interference of reflected/diffracted waves, propagation speed limited by diffusion of seed electrons

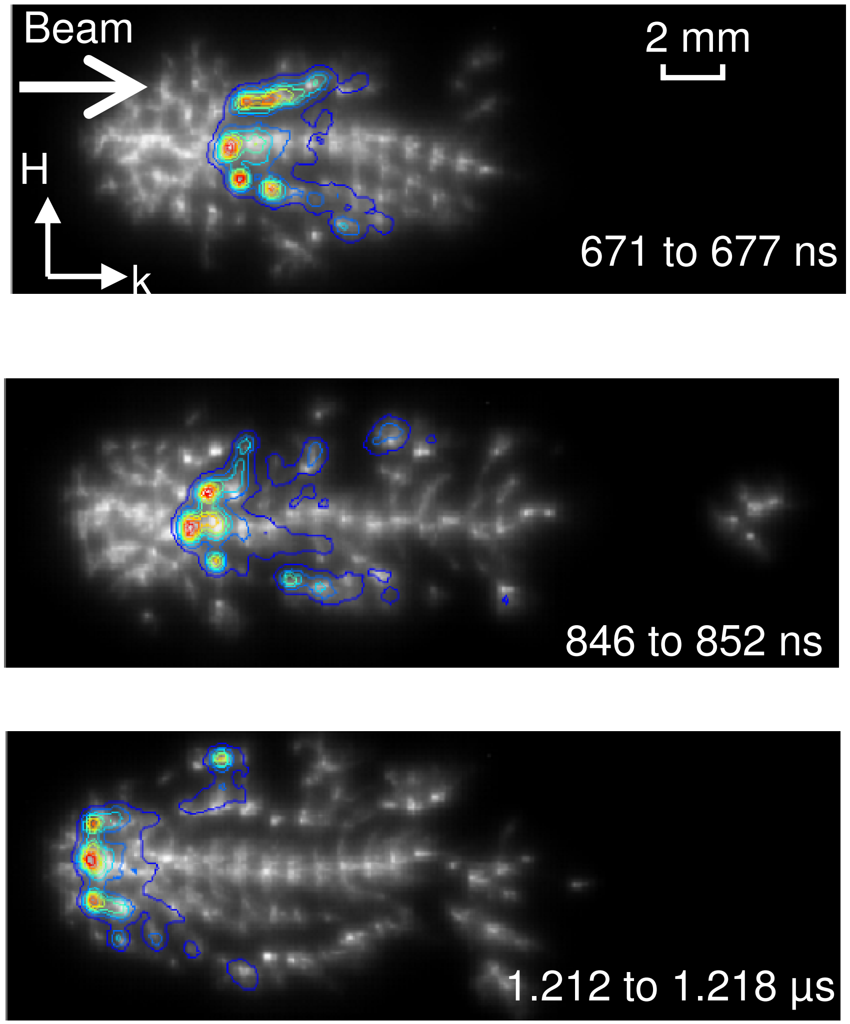

Y. Hidaka, et al., *Phys. Rev. Lett.*, **100**, 035003 (2008).

EM Wave Model

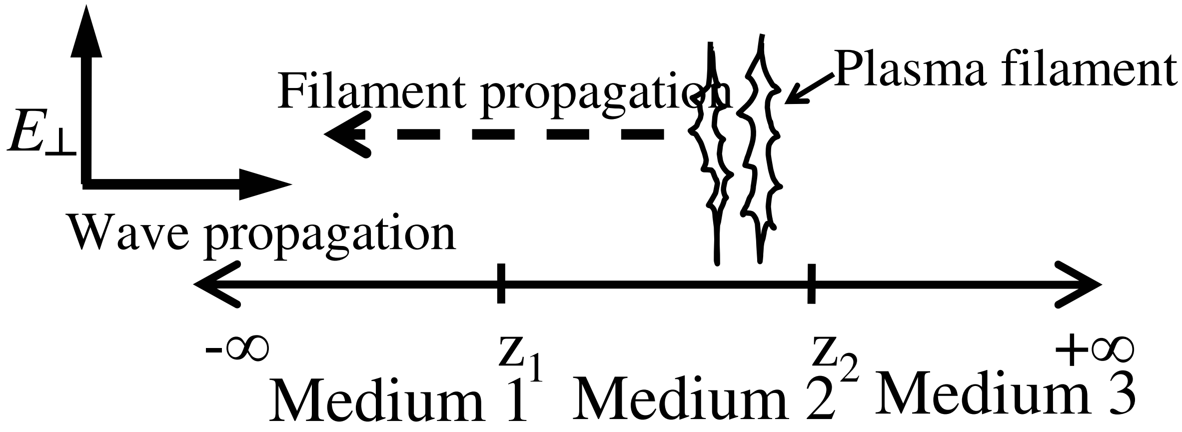

$$\frac{\partial^2 Z}{\partial z^2} + k_z^2 Z = 0$$

$$k_z = k^2 - (k_{x,m}^2 + k_{y,n}^2)$$

$$E_\perp = \mathrm{Re}(E_0 Z e^{-j\omega t})$$

Z is spatial profile of $E_\perp$

vacuum (1 and 3): $$k_1^2 = k_3^2 = \frac{\omega}{c}$$

plasma (2): $$k_2^2 = \frac{\omega}{c}\left(1 - \sum_i \frac{\omega_{p,i}^2(z)}{\omega(\omega + j\nu_{m,i}(z))}\right)^{1/2}$$

$\omega_{p,i}$: plasma frequency

$\nu_{m,i}$: momentum transfer frequency

* H.C. Kim and J. P. Verboncoeur, Comp. Phys. Comm. 177 (2007) 118-121

Fluid Model

Particle Continuity and Electron Energy Equations

$$\frac{\partial n_e}{\partial t} = -\nabla \cdot J_e + K_{ion} n_e n_{gas}, \; J_e = -D_e \nabla n_e - \mu_e n_e E_{\parallel}$$

$$E_{\parallel} = \frac{D_i - D_e}{\mu_i + \mu_e} \frac{\nabla n_e}{n_e}$$

$$\frac{\partial}{\partial t}\left(\frac{3}{2} n_e T_e\right) = -\nabla \cdot q_e + P_{abs} - (\varepsilon_{ion} K_{ion} n_e n_{gas} + \varepsilon_{exc} K_{exc} n_e n_{gas} + \tilde{K}_{mom} n_e n_{gas})$$

$$q_e = -\frac{3}{2} D_e \nabla n_e T_e + \frac{5}{2} J_e T_e$$

$$P_{abs} = \frac{e n_e}{m_e \nu_m} E_{\perp}^2 = \mu_e n_e E_{\perp}^2$$

S. K. Nam and J. P. Verboncoeur, *Phys. Rev. Lett.*, **103**, 055004 (2009)

Filament Simulation Results

E_0 = 5 MV/m, f = 110 GHz, p = 760 Torr t = 6670 T (T = one wave period)

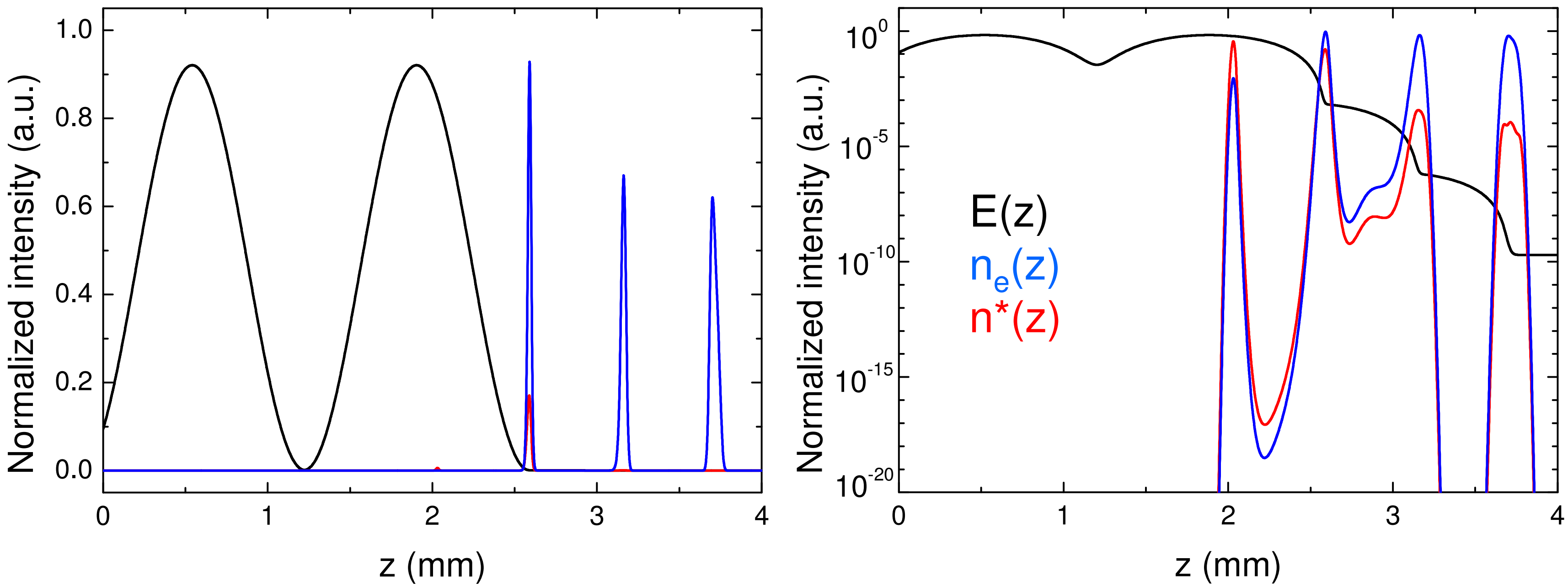

S. K. Nam and J. P. Verboncoeur, *Phys. Rev. Lett.*, **103**, 055004 (2009)

Filament Spacing

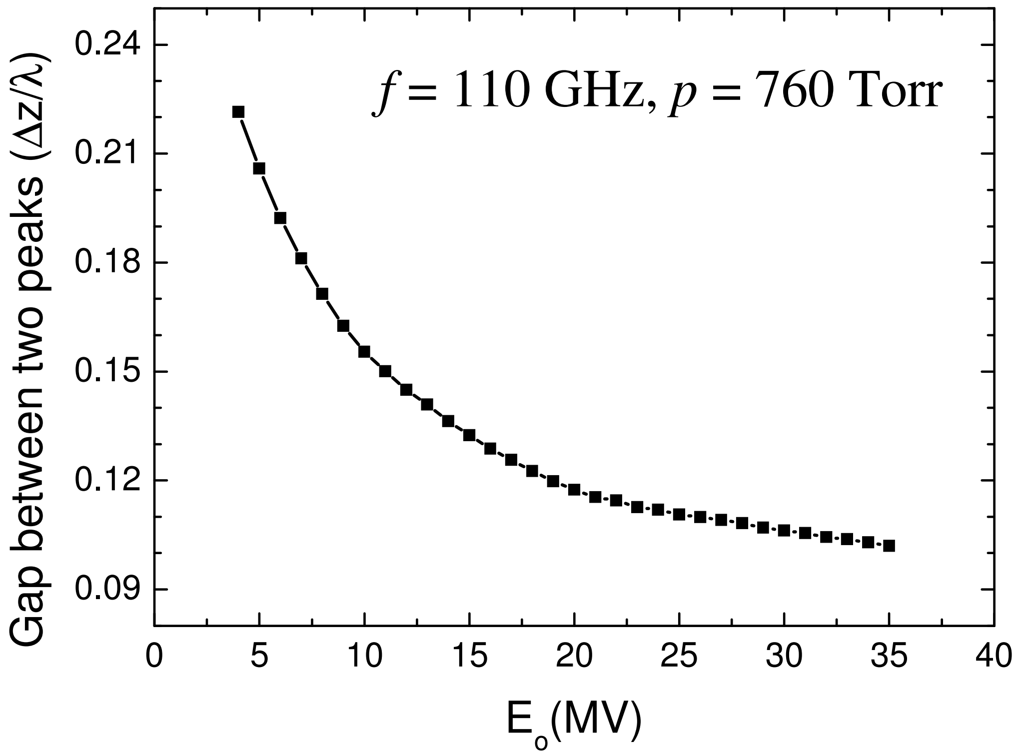

Increasing field strength decreases filament spacing as breakdown threshold is exceeded closer to the previous filament.

Conclusions

- Multipactor dominates at low p
  - No upper field cutoff in waveguide
- Multipactor and ionization discharge compete at intermediate pressure (10-50 Torr)
  - Mean energy decreases with pressure
  - Discharge moves from surface (microns) to volume as pressure increases
  - EEDF goes from bi-Maxwellian to highly cutoff with pressure
- Ionization discharge dominates at atmospheric pressure
- A general scaling law depending on the collision frequency is deduced
- Enhanced kinetic global model agrees with PIC model over 4 orders in pressure, 3 orders in f
  - EEDF shape nearly independent of p, E
  - EEDF shows some dependence on f for Ramsauer gases
- Wave-fluid model reproduces filamentary experiment well
  - Filament distance slightly less than $\lambda/4$
  - Propagation speed ~ ambipolar diffusion